

---

[All ETDs from UAB](#)

[UAB Theses & Dissertations](#)

---

2017

## **An Investigation of the Neurobiological Heterogeneity in Autism, ADHD, and Typical Development**

Melissa Thye  
*University of Alabama at Birmingham*

Follow this and additional works at: <https://digitalcommons.library.uab.edu/etd-collection>

---

### **Recommended Citation**

Thye, Melissa, "An Investigation of the Neurobiological Heterogeneity in Autism, ADHD, and Typical Development" (2017). *All ETDs from UAB*. 3143.  
<https://digitalcommons.library.uab.edu/etd-collection/3143>

This content has been accepted for inclusion by an authorized administrator of the UAB Digital Commons, and is provided as a free open access item. All inquiries regarding this item or the UAB Digital Commons should be directed to the [UAB Libraries Office of Scholarly Communication](#).

AN INVESTIGATION OF THE NEUROBIOLOGICAL HETEROGENEITY IN  
AUTISM, ADHD, AND TYPICAL DEVELOPMENT

by

MELISSA THYE

RAJESH KANA, COMMITTEE CHAIR  
SARAH O'KELLEY  
KRISTINA VISSCHER

A THESIS

Submitted to the graduate faculty of The University of Alabama at Birmingham,  
in partial fulfillment of the requirements for the degree of  
Master of Arts

BIRMINGHAM, ALABAMA

2017

# AN INVESTIGATION OF THE NEUROBIOLOGICAL HETEROGENEITY IN AUTISM, ADHD, AND TYPICAL DEVELOPMENT

MELISSA THYE

LIFESPAN DEVELOPMENTAL PSYCHOLOGY PROGRAM

## ABSTRACT

Standard fMRI studies of healthy as well as clinical populations rely heavily on group-level averages to draw inferences about brain and behavior. This presumes neural and behavioral homogeneity within diagnostic groups resulting in group-level models which may not capture individual variability. This problem is especially relevant for studies of neurodevelopmental disorders such as autism spectrum disorder (ASD) and attention deficit hyperactivity disorder (ADHD) which clinically present with widespread individual differences. The prevalence of comorbidity between these disorders is roughly 28% highlighting the possibility that there may be shared behavioral and neural markers which cut across the diagnostic boundaries delineating the disorders. In order to better characterize these similarities and differences, the current study used a number of data-driven analyses which were blind to diagnostic classification to derive clusters of participants based on functional connectivity among regions within known brain networks. In the first approach, a unified structural equation modeling technique (Group Iterative Multiple Model Estimation) was used to derive subgroups based on connections among regions within three core brain networks: Default Mode, Salience, and Executive Control. For the second analysis, an independent component analysis was used to define components of functionally correlated brain networks. Voxel intensity values were extracted from the component maps of each participant and used in a community detection analysis to identify the community structure of the participants based on

deviations from the group-level components. For the first analysis, 2-3 heterogeneous subgroups were identified for each network, but limitations inherent to the data prevented more robust, generalizable results. Only one cluster was derived from the community detection algorithm, but a number of outlier participants were identified. These results indicate that heterogeneity is a core concern in fMRI analyses and, despite limitations with the data, the analyses presented here provide a useful framework for researchers attempting to conduct neuroimaging analyses that account for individual variability.

Keywords: *Heterogeneity, fMRI, Autism, ADHD, Group Iterative Multiple Model Estimation, Community Detection*

## TABLE OF CONTENTS

	<i>Page</i>
ABSTRACT.....	ii
LIST OF TABLES .....	vi
LIST OF FIGURES .....	vii
CHAPTER	
1 INTRODUCTION.....	1
Clinical Populations .....	2
Brain Connectivity .....	6
Connectivity Based Methods to Study Heterogeneity .....	7
Group Iterative Multiple Model Estimation .....	7
Community Detection.....	9
Independent Component Analysis .....	11
Brain Networks .....	12
Default Mode Network .....	12
Salience Network .....	14
Executive Control Network .....	15
Significance and Innovation .....	16
Specific Aims.....	17
Aim 1 .....	17
Aim 2 .....	18
2 METHODS.....	20
Participants.....	20
Measures .....	23
ABIDE II.....	23
ADHD-200.....	24
Data Analysis .....	25
Scanning Parameters.....	25
Data Preprocessing.....	25
Quality Assurance.....	26
Group Iterative Multiple Model Estimation .....	26
Regions of Interest .....	26

Fit Parameters .....	33
Independent Component Analysis .....	34
Community Detection Analysis .....	36
3 RESULTS.....	37
Overview .....	37
GIMME Analysis .....	37
Default Mode Network.....	38
Executive Control Network.....	39
Salience Network .....	41
ICA and Community Detection Analysis.....	57
4 DISCUSSION .....	62
LIST OF REFERENCES .....	68
APPENDIX: IRB APPROVAL FORM.....	85

## LIST OF TABLES

<i>Table</i>	<i>Page</i>
1 Excluded Participants.....	21
2 Participant Demographics for Matched Sample .....	22
3 Participant Demographics for Full Sample .....	23
4 Modified Shirer Regions of Interest.....	28
5 Spherical Regions of Interest .....	32
6 Participant Subgroup Membership across Modified Thresholds .....	52
7 Demographics for DMN Subgroups .....	53
8 Demographics for ECN Subgroups.....	54
9 Demographics for SN Subgroups.....	55
10 Demographics for Matched Sample Cluster .....	58
11 Outliers.....	59

## LIST OF FIGURES

<i>Figure</i>	<i>Page</i>
1 Shirer ICA-Derived Networks .....	30
2 Spherical Regions of Interest .....	33
3 DMN Group Connectivity Maps.....	43
4 ECN Group Connectivity Maps .....	44
5 SN Group Connectivity Maps.....	45
6 Subgroup Connectivity Maps for the Default Mode Network (.50 threshold) .....	46
7 Subgroup Connectivity Maps for the Default Mode Network (.55 threshold) .....	47
8 Subgroup Connectivity Maps for the Executive Control Network (.50 threshold) .....	48
9 Subgroup Connectivity Maps for the Executive Control Network (.55 threshold) .....	49
10 Subgroup Connectivity Maps for the Salience Network (.50 threshold) .....	50
11 Subgroup Connectivity Maps for the Salience Network (.55 threshold) .....	51
12 Behavioral Demographics across GIMME-Derived Subgroups.....	56
13 Community Detection Derived Clusters for Matched Sample .....	60
14 Community Detection Derived Cluster for Full Sample .....	61



## CHAPTER 1

### INTRODUCTION

Human development is characterized by varied profiles of biological and behavioral outcomes. However, individual variability in both typical and atypical development has largely been treated as noise in standard behavioral and human neuroimaging data analyses which draw inferences from a group-level model. This approach is skewed as it assumes normal distribution of cognitive and neural data across research samples and overlooks the heterogeneity in the sample which is a core issue that affects the reliability and generalizability of fMRI-based inferences (Miller & Van Horn, 2007; Ramsey et al., 2010). This is particularly relevant for researchers attempting to use basic science as a means to inform clinical interventions. The reported results which should serve as the basis for future research and clinical interventions are built upon a model that ignores variability at the individual level. For instance, designing an intervention that targets a group-level deficit in a heterogeneous sample will likely prove only conditionally effective within a subsample of participants that most closely match the group average. Although this homogeneity assumption is especially inflated in clinical populations, it is also problematic in the study of typical development which encompasses wide-ranging developmental outcomes. It is well-established that genetic predispositions and experiences impact an individual's development resulting in unique characteristics and outcomes (Belsky & Pluess, 2009; Bronfenbrenner & Morris, 2007). The non-linear

pattern of human development may introduce the problem of trying to encapsulate “typical” development into a monolithic sample representative of the neurodiversity in the general population. Given the significant heterogeneity within clinical populations as well as across typical development, the present study incorporated data-driven approaches which are blind to diagnostic classification to arrive at subgroups based on neurobiological similarities and differences.

### Clinical Populations

The use of individualized neuroimaging analyses is especially pertinent in studies of neurodevelopmental disorders such as autism spectrum disorder (ASD) and attention deficit hyperactivity disorder (ADHD) which clinically present with widespread individual differences (Lenroot & Yeung, 2013; Wåhlstedt, Thorell, & Bohlin, 2009). ASD is characterized by two core domains: disrupted social communication and restricted and repetitive interests and behaviors (American Psychiatric Association, 2013); and the prevalence of ASD is estimated to be roughly 1 in every 68 children (Center for Disease Control, 2012). ADHD, a separate neurodevelopmental disorder, is diagnosed according to three subtypes: inattentive type, hyperactive/impulsive type, and a combined type. The inattentive type predominately displays symptoms of inattention whereas the hyperactive/impulsive type is characterized by more symptoms of hyperactivity rather than attention. The combined type is diagnosed when a number of both inattentive and hyperactive symptoms are displayed. Similar to the spectrum construct seen in ASD to communicate symptom severity, ADHD diagnosis falls within a mild, moderate, or severe classification depending on the number of symptoms and

disruption to daily functioning (American Psychiatric Association, 2013). The prevalence of ADHD is estimated to be around 6-7% of children and adolescents with the inattentive subtype being the most commonly diagnosed (Willcutt, 2012).

There are several shared characteristics between these diagnostic groups. For instance, both ASD and ADHD are neurodevelopmental disorders with core symptoms emerging in early childhood. Roughly 28% of individuals with ASD are also diagnosed with ADHD (Simonoff et al., 2008) but estimates indicate that between 30-80% of children with ASD and 20-50% of children with ADHD also meet diagnostic criteria for either ADHD or ASD respectively (Rommelse, Franke, Geurts, Hartman, & Buitelaar, 2010). The relatively high incidence of comorbidity between the two disorders highlights the need to further characterize these disorders in tandem due to the possibility of shared or similar etiology. Previous researchers have studied these disorders in conjunction believing that significant insight will be gained by studying the etiological mechanisms contributing to both disorders (Rommelse, Geurts, Franke, Buitelaar, & Hartman, 2011), and have proposed that ADHD and ASD share a similar heritability profile including related genetic traits (Rommelse et al., 2010). In addition, participants with comorbid diagnoses may display a constellation of behaviors that are not characteristic of either disorder (Yerys et al., 2009) suggesting that this comorbid group represents a distinct disorder that requires targeted considerations (Gargaro, Rinehart, Bradshaw, Tonge, & Sheppard, 2011; Leitner, 2014). Some researchers argue for the reconceptualization of ASD and ADHD as different developmental outcomes of a single disorder whereby ASD and ADHD and the comorbid group represent subtypes of the overarching disorder (Brieber et al., 2007; van der Meer et al., 2012). Thus, data-driven algorithms that are

blind to diagnostic classification and provide information about subgroups existing within and across these populations are sensitive to detecting the presence of a shared neurobiological mechanism among participants with either disorder. There may be sub-diagnostic features of ASD that overlap with the behavioral profile of ADHD and vice versa. For instance, problems with attention (Schatz, Weimer, & Trauner, 2002) and in some aspects of executive functioning (Miranda-Casas, Baixauli-Fortea, Colomer-Diago, & Roselló-Miranda, 2013) have been reported by individuals with ASD, and deficits in pragmatic language (Bishop & Baird, 2001) and perspective taking (Marton, Wiener, Rogers, Moore, & Tannock, 2009) have been reported by individuals with ADHD. Furthermore, across participants with ASD and/or ADHD, no consistent demarcations in executive functioning have been found between the two diagnostic groups (Dajani, Llabre, Nebel, Mostofsky, & Uddin, 2016). Thus, there is a significant need to address heterogeneity both within and across these neurodevelopmental disorders.

The variability displayed across participants with ASD and ADHD further underscores the significance of research directed toward disentangling individual differences. It is understood that disorders such as ASD and ADHD are not fully explained by a single gene model, and more recent research efforts have focused on polygenic approaches to studying clinical populations. These approaches are limited, however, in that the variability seen across the severity and symptom expression spectrum in both ASD and ADHD is not fully captured by a single polygenic explanation (An & Claudianos, 2016; Sharp, McQuillin, & Gurling, 2009; Szatmari, 1999). Recent research has supported the idea that different subtypes of neurodevelopmental disorders such as ASD and ADHD display varied genetic profiles; thus, meaningful biological

advances in understanding these disorders necessitates characterizing robust disorder subgroups (Bruining et al., 2010; Jeste & Geschwind, 2014; Sharp et al., 2009).

In ASD specifically, the search for reliable structural or functional brain-based markers has largely been unsuccessful, possibly due to neurobiological variation across the autism spectrum that is not captured by a single biomarker model. For instance, despite a general trend toward a reduction in brain volume differences between ASD and healthy controls with increasing age, many individuals with ASD still display significant structural differences compared to healthy controls across the lifespan (see Lenroot & Yeung, 2013 for review). In addition to biological heterogeneity in genetic mechanisms and brain structure, there are consistent differences in functional activation and connectivity of regions typically associated with the core symptom domains in ASD. In the domain of social cognition, mixed results have been found in ASD populations with atypical activation in the medial prefrontal cortex (Schulte-Rüther et al., 2011), inferior frontal gyrus (Rojas et al., 2006), superior temporal sulcus (Pelphrey, Morris, & McCarthy, 2005), and amygdala (Nacewicz et al., 2006; Schumann, Barnes, Lord, & Courchesne, 2009) which seem to, in part, be driven by the level of symptom severity. Similarly, research on language processing in ASD has suggested general differences in superior temporal gyrus volume (Bigler et al., 2007) and right lateralization of language processing (Herbert et al., 2002) that relates to language comprehension skills. The relation between severity and neurobiological heterogeneity is also seen in the domain of restricted and repetitive behaviors (RRB) where aberrant structural and functional differences in the caudate (Rojas et al., 2006) and dorsolateral prefrontal cortex (Shafritz, Dichter, Baranek, & Belger, 2008) have been shown to relate to RRB severity.

Although there is support for re-conceptualizing ADHD and ASD as emerging from partially shared biological mechanisms, the neurobiological variability in ADHD is typically studied in isolation. The predominant finding in neuroimaging studies of ADHD converges on an aberrant fronto-striatal network, but the extent and behavioral correlates of altered fronto-striatal network functioning in ADHD are not fully understood (Durstun, 2008). In addition, there are conflicting findings regarding volumetric differences in ADHD versus healthy controls in areas such as the caudate, corpus callosum, and cerebellum. These inconsistencies may, in part, be influenced by a similar developmental profile seen in ASD where increased global brain volume is noted in early development, but these volumetric differences decrease over time (Valera, Faraone, Murray, & Seidman, 2007). Similar to studies on ASD, the level of symptom severity relates to the presence and degree of altered structural and functional connectivity findings in ADHD (Castellanos, Sonuga-Barke, Milham, & Tannock, 2006). A lack of convergence may stem from a failure to account for symptom severity in both behavioral and neuroimaging studies. Similar to ASD, meaningful subtyping has not been successful in ADHD research. Thus, there is significant neurobiological diversity that extends from genetic heterogeneity to individual differences in brain function and structure within ASD and ADHD populations that has traditionally been studied as noise rather than an outcome of interest.

### Brain Connectivity

Although the field of fMRI research has historically relied on areas of brain activation to understand and interpret cognitive processes, more complex models of

human brain functioning provide information about the brain and behavior. Such models offer insight into activation across time, spatial distance, and brain region thus facilitating a more complex and sophisticated understanding of large-scale brain networks (Smith, 2012). Functional connectivity provides information about the synchronous connections between and among different brain regions and helps elucidate the role of brain networks in normal and pathological conditions (van den Heuvel & Hulshoff Pol, 2010; Van Dijk et al., 2010). Thus, connectivity analyses are able to discern patterns of regional recruitment across the brain in a way that standard functional activation analyses cannot. With a goal of deriving subgroups of participants based on shared neural mechanisms regardless of diagnostic label, the present project used functional connectivity as the primary neural index. Specifically, intrinsic functional connectivity, measured when the brain is at rest, provides insight into baseline brain functioning that can be predictive of cognitive performance (Grady et al., 2010; Shirer, Ryali, Rykhlevskaia, Menon, & Greicius, 2012). Therefore, connectivity analyses allow for a comprehensive network-level examination of brain functioning.

### Connectivity Based Methods to Study Heterogeneity

#### *Group Iterative Multiple Model Estimation*

Although there are numerous methods to study functional connectivity (see Mumford and Ramsey, 2014 for review), a relatively recent approach addresses the problem of ignoring within-group heterogeneity implicit to standard fMRI analyses. The *Group Iterative Multiple Model Estimation* (GIMME) algorithm adopts a unified structural equation modeling (uSEM) framework to derive both a group-level

connectivity map that is optimally suited for the majority of the group as well as individual-level connectivity maps that further characterize each participant. Using a simulated dataset, this method has been shown to reliably recover both the presence and direction of connections among regions within a network (Gates & Molenaar, 2012). The GIMME algorithm runs a null network on all of the participants to identify the connectivity map that best represents the group. This is accomplished by examining which paths, if freed from the model, would optimize the fit of the model for the group. If paths are included in the group model that are not reflective of a significant portion of the individuals, they are removed from the group-level model. The default group-level threshold in GIMME (e.g. .75 or 75% of the group) has been used in other neuroimaging research (van den Heuvel & Sporns, 2011) and is thought to capture the majority of the group. After this optimized group-level connectivity map is established, the GIMME algorithm then applies this map to the individual level in a semi-confirmatory analysis to assess if there are pathways that, if added, will improve the fit of the individual-level model. The connectivity model is then optimized at the individual level, although no pathways that were present in the group-level analysis are removed from the individual models. A final confirmatory analysis is run to assess individual model fit (see Gates & Molenaar, 2012 for review of method). If the individual-level connectivity maps for participants are similar, the algorithm will cluster participants into subgroups and output a subgroup-level connectivity profile which characterizes the members of the subgroup. If no convergence among individual-level connectivity maps exists, the algorithm does not force subgroups to emerge. Building upon standard connectivity analyses, which recover the presence of the connection, as well as effective connectivity approaches,



which provide information about the direction of the connection, adopting a uSEM approach to calculate the presence and direction of pathways has been suggested to be a more robust alternative to standard non-SEM based connectivity approaches (Gates, Molenaar, Hillary, Ram, & Rovine, 2010). In deriving functional connectivity maps of each participant, GIMME primarily relies on contemporaneous connections across the regions. However, the model also accounts for lagged connections which allows for the detection of autocorrelations of each region with itself to arrive at a more reliable outcome. Previous attempts to study brain connectivity within a uSEM framework have been found to be successful, and this method offers an ideal solution to uncovering the presence and directionality of neural pathways (Kim, Zhu, Chang, Bentler, & Ernst, 2007). Thus, the novelty of the statistical model adopted by the GIMME algorithm coupled with the sensitivity to individual variation make this a promising approach to study heterogeneity in intrinsic functional connectivity across typical development and clinical populations.

### *Community Detection*

Community detection is a statistical approach that is grounded in graph theory which applies mathematical constraints to uncover the community structure within a dataset. The Girvan-Newman community detection algorithm (Girvan & Newman, 2002) relies on four network principles to recover communities within the dataset: 1) small world property, originally developed through the study of social networks (Milgram, 1967), posits that the connections among a set of nodes (or vertices) within a network are short and the number of edges required to travel from one node to another node is relatively

few. This property is typically quantified by taking the logarithmic function of the total number of nodes in a given network; 2) power-law degree distributions describe a scale-free network where nodes that are added to a given network preferentially attach to nodes that are well connected (e.g. hubs). Typically, the number of well-connected nodes is small, and a power law constrains the relationship between the introduction of new nodes and the connections to well-established nodes. Modifying one feature inadvertently impacts the other in a systematic way. This property suggests that an organizational principle dictates the connection of nodes to established hubs and is considered an alternative to a randomly organized network (Amaral, Scala, Barthelemy, & Stanley, 2000; Barabasi & Albert, 1999); 3) network transitivity (e.g. clustering) describes the principle where nodes that share a neighboring node are more likely to be neighbors themselves (Newman, Strogatz, & Watts, 2001). This principle forms the basis of how nodes are clustered together; 4) community structure defines the relationships among the identified communities within a given network. For instance, communities of dense connections are connected to other, distant communities through relatively sparse connections.

The Girvan-Newman community detection algorithm relies on the edge-betweenness centrality metric to identify the underlying community structure (Girvan & Newman, 2002; Newman, 2004). Relying on the efficiency principle that information will tend to travel over the shortest path, betweenness centrality examines the influence of a given edge by counting the number of short paths connecting other nodes that run along the examined edge. The edges with the highest edge betweenness are then progressively removed from the network and the consequences of their removal are quantified by

recalculating the betweenness centrality of the remaining edges. The edges with the highest betweenness centrality are likely those edges that connect distant communities as the number of edges available to travel along are sparse resulting in a higher number of connections. When these edges are removed only the identified communities (e.g. groups) remain. This algorithm has been shown to accurately recover the community structure in simulated networks (Girvan & Newman, 2002) and has been applied to varied data types ranging from neuropsychological measures (Fair, Bathula, Nikolas, & Nigg, 2012; Karalunas et al., 2014) to functional brain networks (Meunier, Achard, Morcom, & Bullmore, 2009; Wang et al., 2009) making this approach flexible and applicable to data with a complex network structure.

### *Independent Component Analysis*

Independent component analysis (ICA) is uniquely suited to multidimensional fMRI data. ICA breaks down the multivariate signals inherent to fMRI and extracts the signal from each voxel. This signal is subsequently analyzed as an independent function from all other voxels. The result is the isolation of spatially independent components. The benefit of this analytic approach is that ICA can recover signals that would be excluded or inappropriately modeled if a Gaussian distribution is assumed (Calhoun, Pearlson, & Adali, 2004; McKeown et al., 1998). When provided with resting-state fMRI data, the ICA derives group-level spatially independent components which reflect brain regions or networks with shared time-courses. Thus, this analysis is a measure of functional connectivity. In the present study, ICA was conducted on the data from all participants (ADHD, ASD, and TD) together as a large group. This resulted in components that best

represent the entire group of participants. The participant z-scores indicating the fit of each component at the individual level were then statistically analyzed using the Girvan-Newman community detection algorithm to cluster participants into communities. The novelty of this analytic approach is the use of a rigorous statistical pipeline that is blind to diagnostic and behavioral information.

## Brain Networks

### *Default Mode Network*

The Default Mode Network (DMN) is the primary brain network that is active during rest and provides a large-scale understanding of baseline neuronal activity (Greicius, Krasnow, Reiss, & Menon, 2003). Measuring the intrinsic functional connectivity (e.g. connectivity during rest) provides valuable information about the spontaneous fluctuations of this brain network which can be broadly informative in elucidating the role of this network in other cognitive processes. Although the DMN is shown to be active during rest, it is not a passive network and rather serves an important role in the various cognitive processes including self-referential thinking, ToM processing, and memory retrieval (Andrews-Hanna, Smallwood, & Spreng, 2014). Successful modulation of the DMN from passive to active processing also impacts cognitive performance and has been shown to be disrupted in clinical populations such as ASD (Kennedy, Redcay, & Courchesne, 2006). For instance, altered connectivity within this network has been implicated in ASD and related to the social deficits inherent to the disorder (Lynch et al., 2013; Yerys et al., 2015). Deficits in DMN up-regulation (Sidlauskaite, Sonuga-Barke, Roeyers, & Wiersema, 2016b) and altered connectivity

within DMN has also been noted in ADHD (Sidlauskaite, Sonuga-Barke, Roeyers, & Wiersema, 2016a). Thus, examination of the connectivity profile of DMN during resting-state may provide insight into clinical populations with suspected DMN abnormalities.

Disrupted DMN connectivity has been widely reported in ASD and it has been suggested as an endophenotype of the social deficits characteristic of ASD (Yerys et al., 2015). An ICA analysis revealed decreased functional connectivity across DMN regions which was related to the severity of social symptoms as measured by the Autism Diagnostic Observational Schedule (ADOS) and the Social Responsiveness Scale (SRS; Assaf et al., 2010). The maturation of DMN connections is also delayed in many individuals with ASD compared to typically developing peers who establish functional connections among the regions of the DMN between the ages of 11-13 (Washington et al., 2014). There have also been consistent reports of reduced activation during social processing in the prefrontal cortex and posterior superior temporal sulcus which are nodes within the DMN (Dichter, 2012).

Children with ADHD generally display an underdeveloped brain with structural abnormalities noted in core regions of the DMN such as reduced volume in the ACC and dorsolateral prefrontal cortex (DLPFC; Moreno-Alcázar et al., 2016). Individuals with ADHD also have trouble modulating between task and rest as evidenced by activation of DMN during task (Sidlauskaite et al., 2016b). Additional research suggests that individuals with ADHD are hyperconnected to various networks during rest including the DMN (Sidlauskaite et al., 2016a). Thus, there are numerous reports of altered intrinsic connectivity of regions comprising the DMN in both ASD and ADHD populations.

### *Saliience Network*

In addition to the DMN, two additional networks have been proposed to be critical in studying cognition in both typical and clinical populations (Menon, 2011): the salience network (SN) and the executive control network (ECN). The salience network is involved in attending to stimuli in the environment by selectively detecting and filtering out relevant and superfluous information. The SN is also involved in integrating information, and is thus a critical system for a variety of executive functions and behavioral tasks (Seeley et al., 2007). Research suggests that the SN is altered in a variety of clinical disorders ranging from schizophrenia to anxiety disorders (see Menon, 2011 for review). Using a trained classifier, researchers have been able to accurately distinguish ASD versus TD individuals based on hyperactivity of the SN (Uddin et al., 2013). However, there are conflicting reports of SN functioning with some studies reporting SN hypoconnectivity in ASD (Abbott et al., 2016). Inconsistencies in the reported connectivity profiles in ASD may suggest that heterogeneity exists in SN functioning across individuals with ASD, and the analyses proposed here are sensitive to detecting such differences and potentially reconciling these conflicting findings. In ADHD, connectivity differences are seen between the SN and other intrinsic brain networks which distinguish participants with ADHD from typical controls (Sidlauskaite et al., 2016a). Given the importance of this network in investigations of psychopathology and the previous research findings of altered SN connectivity in both ASD and ADHD, the current study investigated whether connectivity among core SN regions is altered in ASD and ADHD in any systematic or overlapping way.

### *Executive Control Network*

The last network that is proposed to be broadly impacted across clinical populations is the executive control network (e.g. fronto-parietal control network) which is involved in a wide-range of functions including working memory, goal-directed behavior, decision making, and problem solving (Menon, 2011). The role of the ECN in a variety of cognitive tasks underscores the importance of studying this network and identifying whether deficits inherent to the ECN result in specific cognitive or behavioral impairments downstream. In ADHD, regions within this network have been consistently reported as hypoactive in response to both inhibition tasks such as go/no go and attentional tasks (Castellanos & Proal, 2012) which aligns with the characteristically poor behavioral performance of individuals with ADHD within these cognitive domains. Interestingly, altered ECN connectivity has also been reported in ASD, but, unlike individuals with ADHD, recent findings indicate that individuals with ASD are characterized by hyperconnectivity between the ECN and other intrinsic brain networks such as the DMN (Abbott et al., 2016). In addition, intrinsic functional connectivity within the DMN, SN, and ECN has been shown to predict long-term outcomes of ASD symptom progression beyond what standard behavioral batteries are able to predict (Plitt, Barnes, Wallace, Kenworthy, & Martin, 2015). There are varied findings across both ASD and ADHD and a lack of research investigating these three core networks with a sample of ASD, ADHD, and TD participants in conjunction. Thus, the current study sought to understand how these networks relate to behavioral profiles and to determine whether connectivity profiles among these networks cluster along diagnostic boundaries.

## Significance and Innovation

The proposed project used a novel, multifaceted data-driven approach to classifying participants into subgroups based on brain connectivity (not on clinical diagnosis) which is a departure from standard fMRI analyses. Identifying subgroups that include participants with different diagnostic labels has the potential to highlight shared neural patterns that can account for comorbidity in clinical diagnoses in a way that has not been previously considered. Although previous researchers have examined these disorders in tandem, this is the first study, to our knowledge, which targeted heterogeneity within and among ASD, ADHD, and TD populations using an individualized GIMME framework as well as a unique application of ICA and community detection.

The Research Domain Criteria (RDoC) Initiative of the National Institute of Health (NIH) aims to encourage the study and application of analyses to identify shared mechanisms across diagnostic groups. The present study directly addressed this initiative by studying the shared and differential neural mechanisms of three groups traditionally studied as mutually exclusive: ASD, ADHD, and typical development. This study is novel and innovative as it adopted data-driven, individualized approaches to classification that are grounded in brain connectivity rather than behavioral observation. This approach further challenges researchers and clinicians alike to re-conceptualize human brain and behavior as an all-encompassing spectrum with individuals with both typical and divergent development falling at different points along a single continuum. The subgrouping of individuals with ASD or ADHD based on brain connectivity can provide clinicians with a better understanding of underlying neural deficits that are associated with core diagnostic behaviors which can be further used to predict response



to treatment and to individualize treatment planning. The inclusion of typically developing participants allows researchers to identify individuals with a sub-diagnostic behavioral profile, but shared neural mechanisms of a given disorder like ASD or ADHD. This can provide important information about compensatory behaviors or neurobiological mechanisms that can directly impact intervention design and treatment planning for at-risk individuals. Data analysis that prioritizes the individual over the group provides increased specificity about subtypes within a clinical population. Human development is heterogeneous and applying a model that forces group level uniformity at best relies on assumptions that are flawed and at worst disseminates research that directly informs clinical interventions that are ineffective for a large portion of individuals within a given diagnostic group and perpetuates an oversimplified representation of human functioning.

### Specific Aims

The present project examined the common and differential patterns of brain connectivity across participants regardless of diagnostic status using two distinct, but complementary methodological aims:

#### *Aim 1*

Subgroup participants across groups of clinical (ASD and ADHD) and non-clinical (typical development) populations based on connections among *a priori* regions of interest within known networks (DMN, ECN, SN) regardless of diagnostic classification.

This aim was accomplished by applying the GIMME algorithm to resting-state fMRI data to derive group-level, subgroup-level, and individual-level functional

connectivity maps among *a priori* regions of interest within the DMN, SN, and ECN. The data were analyzed using the freely available R package (gimme; Lane et al., 2015).

*Hypothesis 1.* It was hypothesized that subgroups would emerge that differed from the group-level model, and these subgroups would consist of individuals from both clinical populations studied due to the comorbidity between ASD and ADHD (Simonoff et al., 2008). Reduced connectivity across all three networks was expected in the subgroups containing the largest percentage of ASD and ADHD participants.

#### *Aim 2*

Apply a community detection algorithm to brain connectivity data to cluster participants into groups based on variations from ICA-derived group-level components.

This aim was accomplished by using the freely available Group ICA of fMRI Toolbox (GIFT; <http://www.nitrc.org/projects/gift>) to conduct a whole-brain independent component analysis of the resting state data from all participants to arrive at both group-level and individual-level components comprised of temporally correlated, spatially distinct regions. The group-level components were then used as binarized masks to extract average or thresholded z-scores from the corresponding individual-level component maps. These z-scores are a reflection of the average contribution of the voxels to each component and were used in a Girvan-Newman community detection algorithm to derive the community structure among the participants. Unlike the first aim, this analysis did not rely on *a priori* regions of interest to ascertain subgroups which allows

component maps to incorporate regions outside of those specified in aim 1 which can highlight patterns of atypical connections outside of the DMN, SN, or ECN.

*Hypothesis 2.* It was hypothesized that clusters of participants would be derived, due to the heterogeneity in the sample, and that these clusters would correspond to the subgroups identified using the uSEM GIMME algorithm. Additionally, it was hypothesized that clusters which contain the largest percentage of ASD and ADHD participants would be characterized by individual-level components with the greatest deviation from the group-level component maps.

## CHAPTER TWO

### METHODS

#### Participants

The data for the present study were taken from both the Autism Brain Imaging Data Exchange II (ABIDE II: [http://fcon\\_1000.projects.nitrc.org/indi/abide/](http://fcon_1000.projects.nitrc.org/indi/abide/); Di Martino et al., 2014) and the ADHD-200 databases ([http://fcon\\_1000.projects.nitrc.org/indi/adhd200/](http://fcon_1000.projects.nitrc.org/indi/adhd200/)) which are publically available larger repositories of structural and resting state MRI data. The data collected at Oregon Health & Science University from the ABIDE II and ADHD-200 databases were used due to correspondence between the scanner and scanning parameters. All participants in both datasets were instructed to withhold the administration of psychostimulant drugs or other medications for at least 24 hours prior to scanning. Only participants who were instructed to keep their eyes open were used in this analysis as past research has illustrated the varying effects of eyes open versus eyes closed during resting state (Patriat et al., 2013).

Prior to excluding participants based on motion and data quality, there were 172 participants (37 ASD; 37 ADHD; 98 TD) between the ages of 7 to 15 years. Data from ABIDE I were not used due to the overlap in TD participants between the ABIDE I and ADHD-200 databases. Additionally, unlike the ABIDE II and ADHD-200 sample, participants included in the ABIDE I database did not complete the entire WISC-IV assessment. A total of 43 participants were excluded due to motion or data quality

resulting in a final sample of 129 participants. The ADHD participants who were excluded did not significantly differ in age or on any of the available measures (e.g. ADHD subscales, IQ) when compared to the retained participants. See Table 1 for information about excluded participants.

Table 1.

*Excluded Participants*

Exclusion Criteria	Group	ABIDE II	ADHD-200
>20% time points exceed .5mm	TD	6	12
	ASD	5	-
	ADHD	-	13
Visual quality assurance	TD	0	3
	ASD	0	-
	ADHD	-	4
Total		11	32

*Note:* TD = Typically Developing; ASD = Autism Spectrum Disorder; ADHD = Attention Deficit Hyperactivity Disorder.

After excluding participants, the remaining sample was not evenly divided among the diagnostic groups (77 TD; 32 ASD; 20 ADHD). The analyses utilized in this project are data-driven such that models are derived from the entire sample of data without *a priori* knowledge concerning diagnostic classification. Therefore, in order to avoid overweighting the models with typically developing participants and to address a potential confound where the TD group had more power and influence, the participant groups were limited to a final sample of 20 participants per diagnostic group. Additionally, the groups were only matched on IQ because the ASD participant group

was older on average compared to either the TD or ADHD groups. To allow for a more thorough investigation of the heterogeneity among the full sample of participants, the analyses for aim 2 were performed on the matched sample group (n = 60) as well as the full sample group (n = 129) with the understanding that there are significant limitations to both approaches in isolation. When excluding ASD participants for the matched sample group, the excluded participants did not differ from the retained participants on any of the available autism measures (e.g. ADOS-2, ADI-R, SRS) and were excluded based only on IQ and age. Age of the participants was the only significant difference between the final matched sample ASD group and the ASD participants who were excluded from the sample. Additionally, the TD group in the matched sample were comprised of 10 participants from ABIDE II and 10 participants from ADHD-200. See Table 2 and Table 3 for demographic information on the matched and full sample of participants respectively.

Table 2.

*Participant Demographics for Matched Sample*

	TD	ASD	ADHD	<i>F</i>	<i>p</i>
N	20	20	20	-	-
Age (SD)	9.67 (1.18)	10.90 (1.77)	9.04 (1.17)	9.11	<.01
IQ (SD)	111.55 (11.33)	109.35 (14.34)	111.30 (11.76)	.184	.83
Gender (M:F)	14:6	17:3	14:6	-	-

*Note:* TD = Typically Developing; ASD = Autism Spectrum Disorder; ADHD = Attention Deficit Hyperactivity Disorder; SD = Standard deviation of the mean. M = Male; F= Female.

Table 3.

*Participant Demographics for Full Sample*

	TD	ASD	ADHD	<i>F</i>	<i>p</i>
N	77	32	20	-	-
Age (SD)	9.94 (1.69)	11.63 (2.30)	9.04 (1.17)	15.01	<.01
IQ (SD)	117.71 (12.57)	106.28 (17.85)	111.30 (11.76)	8.00	<. 01
Gender (M:F)	43:34	26:6	14:6	-	-

*Note:* TD = Typically Developing; ASD = Autism Spectrum Disorder; ADHD = Attention Deficit Hyperactivity Disorder; SD = Standard deviation of the mean. M = Male; F= Female.

Measures

*ABIDE II*

To confirm diagnosis, participants were administered the third module of the Autism Diagnostic Observation Schedule – Second Edition (ADOS-2; Lord et al., 2012). The ADOS-2 contains subscales measuring restricted and repetitive behaviors (RRB), social affect, and severity of symptoms, and provides a total score. Module 3 is given to children who are verbal, and higher scores on all of these measures indicate greater impairment within that domain with social affect scores greater than 8 and a total score greater than 9 indicating ASD (Gotham, Risi, Pickles, & Lord, 2007). Parents completed the Autism Diagnostic Interview-Revised (ADI-R; Lord et al., 1994) and the Social Responsiveness Scale – Second Edition (SRS-2; Constantino & Gruber, 2012). The ADI-R is a structured interview assessment which contains questions regarding the development of the participant across several domains including social development, presence of restricted and repetitive behaviors, and communication. A social interaction

score greater than 10, a verbal communication score above 8, and a restricted and repetitive behavior score above 3 are the ASD cutoff scores. The SRS is a measure of ASD traits administered to children and adults which has five subscales: social awareness, social cognition, social communication, social motivation, and restricted and repetitive interests. On each of the subscales, a T-score below 59 is considered typical, a T-score from 60 to 65 indicates mild impairment, a T-score from 66 to 75 indicates moderate impairment, and a T-score greater than 76 suggests severe impairment. Participants were given the three-subtest short form (Block Design, Vocabulary, and Information) of the Wechsler Intelligence Scale for Children – Fourth Edition (Wechsler, 2003) and were excluded if their estimated IQ was below 70. The researchers did not explicitly exclude ASD participants who had comorbid diagnoses.

#### *ADHD-200*

Parents of each of the participants were administered the Conners' Parent Rating Scale-Revised, Long version (CPRS-LV; Conners, 1997) which is an ADHD symptom checklist. Inclusion into the ADHD group required a T-score greater than 65 on at least one of the ADHD subscales of the CPRS-LV, whereas inclusion in the typically developing group required a T-score below 60 for the Inattentive and Hyperactive/Impulsive scales on the CPRS-LV. All participants were administered the Wechsler Abbreviated Scale of Intelligence (WASI; Wechsler, 1999), and were excluded if their Full Scale Intelligence Quotient (FSIQ) was below 80. ADHD participants were excluded if they had a comorbid ASD diagnosis.



## Data Analysis

### *Scanning parameters*

Resting-state data from both ABIDE II and ADHD-200 were acquired using the 3T Siemens Magnetom TrioTim scanner at Oregon Health & Science University. Structural MRI T1-weighted scans were acquired using a MPRAGE (Magnetization Prepared Rapid Acquisition Gradient Echo) sequence with the following parameters: repetition time (TR) = 2300ms, echo time (TE) = 3.58ms, field of view (FOV) = 256 x 240, 1.0mm isotropic voxels, flip angle = 10°. The resting state data were acquired using an interleaved sequence with the following parameters: TR = 2500ms, TE = 30ms, FOV = 240 x 240, 3.8mm isotropic voxels, flip angle = 90°.

### *Data Preprocessing*

Functional images were preprocessed using Analysis of Functional NeuroImages (AFNI; Cox, 1996) and FMRIB Software Library (FSL; Smith et al., 2004). The FAST automated segmentation program implemented in FSL was used to skull strip and segment the white matter, cerebrospinal fluid (CSF), and grey matter in the raw anatomical images which were then bias corrected and nonlinearly transformed into MNI space. Functional images were motion-corrected by registering each functional volume to the middle time point in the scan, co-registered with the anatomical, normalized and resampled to a 3mm isotropic MNI template, smoothed with a 6mm Gaussian kernel, and bandpass filtered ( $0.008 < f < 0.08$  Hz). Nuisance variables (e.g. white matter, CSF, the 6 rigid-body motion regressors, and the derivatives of these variables) were deconvolved with the processed functional volumes resulting in a total of 16 nuisance regressors.

### *Quality Assurance*

Participant head motion during scanning can result in artefacts and data distortion and is a significant concern in functional connectivity analyses (Satterthwaite et al., 2012; Van Dijk, Sabuncu, & Buckner, 2012). To account for this problem, the Euclidean distance from the six rigid-body motion parameters (three rotation parameters: roll (y axis), pitch (x axis), yaw (z axis); three translation parameters along the x, y, and z axes) was calculated across the time points and any shift greater than .5mm was deemed excessive head motion. Participants with greater than 20% of time points exceeding this motion threshold were excluded from the subsequent analyses (n = 36). Time points where motion exceeded the desired cut-off of .5mm were not censored because the analyses required equal data across all participants.

In addition to accounting for head motion, a rigorous quality assurance pipeline was used which involved visually inspecting the raw and final preprocessed anatomical and functional data for each participant. Participants with artefactual raw data or poorly registered functional or anatomical volumes were excluded from the subsequent analyses (n = 7).

### **Group Iterative Multiple Model Estimation**

#### *Regions of Interest*

GIMME uses the time series from regions of interest (ROIs) to build a model of connectivity which derives both the presence and direction of connections among the specified regions. Initially, the ROIs were derived from the Shirer group (Shirer, Ryali, Rykhlevskaia, Menon, & Greicius, 2012) which identified important intrinsic networks in

the brain by applying ICA to resting state data from typically developing participants. These functionally derived regions were used due to the interest in studying large scale networks across the participant groups. Additionally, the use of purely anatomical regions would have constrained the analysis to structural boundaries which ignores information regarding the functional recruitment of regions within a network. Recent research has highlighted the need to incorporate information from multiple levels (e.g. function, architecture, connectivity, and topography) to identify new, more informative boundaries in the brain (Glasser et al., 2016).

Despite the advantages of using ROIs derived from information regarding functional connectivity, there were a number of limitations. The ROIs varied significantly in size across the networks ( $SD = 682-1478$  voxels). This has direct implications when averaging the time series of voxels within each ROI. Voxels within smaller regions would contribute significantly to the ROI average, whereas voxels within larger ROIs would have relatively less contribution. Additionally, differences in ROI size introduces varied levels of susceptibility to noise and degrees of power to detect the real signal. Many of the Shirer ROIs from the same network overlapped which created a problem where some voxels were contributing to multiple regions. To partially address these concerns, the regions from the Shirer lab were modified in the following ways. First, regions with fewer than 50 voxels were excluded ( $n = 4$ ). Second, overlapping voxels from regions within the same network were removed from the larger region and were retained in the smaller region. Thus, the time series from the voxels only contributed to whichever region initially had fewer voxels. Third, regions that were considered irrelevant or less crucial to the network were removed when necessary (DMN: Right Lobule IX, Left

Middle Occipital Gyrus; SN: Left and Right Lobule VI, Crus I). Fourth, similar regions were combined (DMN: Left and Right Hippocampus, Left and Right Parahippocampus; SN: Left Middle Frontal Gyrus). Fifth, regions that were exceedingly large were reduced in size. This occurred with the MPFC region in the DMN ( $k = 5,257$ ). To avoid discarding this ROI due to the role of the MPFC in this network, the ROI was broken into two smaller regions. This was done using the Automated Anatomical Labeling atlas (AAL; Tzourio-Mazoyer et al., 2002) to define a structural ROI for the regions comprising the larger functionally defined ROI. The regions chosen in the atlas were "Frontal\_Sup\_Medial (bilateral)" and "Frontal\_Med\_Orb (bilateral)". The structural ROIs were then individually multiplied by the larger functional ROI to derive a mask of overlapping voxels. Visual examination suggested that these new structural/functional hybrid regions appeared to capture the approximate area of the original functional ROI. The approach adopted here is preferable to using the unaltered structural ROIs because research has shown functionally defined regions of interest to be more informative when studying continuous cognitive states such as in resting-state analyses (Shirer et al., 2012). Thus, this ROI is a structural/functional hybrid that shows correspondence between a strictly structural or strictly functional approach. After modifying the ROIs, there were 15 regions for the DMN, 14 for the SN, and 11 for the ECN (Table 4 and Figure 1).

Table 4.

*Modified Shirer Regions of Interest*

Region	Hemisphere	No. of Voxels
<b>Default Mode Network</b>		
Medial Prefrontal Cortex	-	2153
Precuneus	-	1921

Posterior Cingulate Cortex	-	1390
Orbitofrontal Cortex	-	891
Angular Gyrus	Right	752
Retrosplenial Cortex	Right	590
Hippocampus	-	510
Retrosplenial Cortex	Left	462
Middle Frontal Gyrus	Left	405
Middle Frontal Gyrus	Right	399
Parahippocampal Gyrus	-	224
Thalamus	-	220
Superior Frontal Gyrus	Right	137
Midcingulate Cortex	-	114
Angular Gyrus	Left	97

### **Executive Control Network**

Crus I	Left	2403
Inferior Parietal Gyrus	Left	2110
Superior Frontal Gyrus	Right	2093
Inferior Parietal Gyrus	Right	1873
Middle Frontal Gyrus	Left	1501
Inferior Frontal Gyrus	Left	437
Middle Frontal Gyrus	Right	356
Middle Temporal Gyrus	Left	350
Crus I	Right	310
Caudate	Right	188
Superior Medial Gyrus	Right	83

### **Salience Network**

Anterior Cingulate Cortex/ Supplementary Motor Area	-	2887
Inferior Parietal Lobule	Left	1205
Inferior Parietal Lobule	Right	1002
Middle Frontal Gyrus	Left	741
Middle Frontal Gyrus	Right	470
Insula	Right	319
Insula	Left	305
Thalamus	Left	142
Posterior Insula	Right	134
Precuneus	Right	133
Posterior Insula	Left	114
Precuneus	Left	98
Thalamus	Right	63
Midcingulate Cortex	Right	56

---

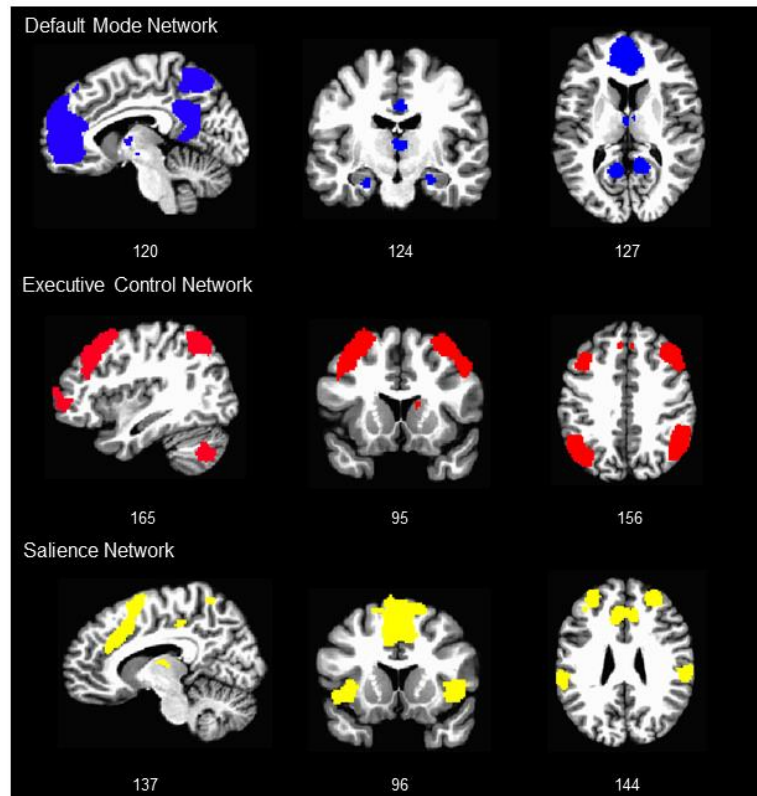


*Figure 1.* Shirer ICA-Derived Networks.

There were two significant methodological concerns that resulted in the group and individual models not converging when using the modified Shirer ROIs. First, there was an insufficient number of time points in the data (e.g. 78) to model connectivity among the regions of interest (S. Lane, personal communication, July 24, 2017). The maximum number of regions for a given network was 15, but GIMME accounts for both lagged and contemporaneous connections which results in a total of 30 variables that are fit to the data. Standard structural equation modeling analyses require a sample size of at least 10 observations or time points per variable (Bentler & Chou, 1987). With 15 regions of

interest, a minimum suggested requirement is approximately 150 observations or time points which is almost twice the number of data points in the current study. In a standard SEM framework, when the number of observations is insufficient, the fit indices will be poor. However, GIMME uses an iterative SEM procedure to optimize fit indices by adding and removing paths until the fit indices pass an acceptable threshold indicating good model fit. In this case, the fit indices were never able to surpass this threshold despite adding all possible paths, and the program terminated before providing any results. The second problem with the modified Shirer ROI analysis was the degree of multicollinearity among the ROI time series ( $r > .80$ ) suggesting that these variables should be dropped or used as composite variables by merging regions together (S. Lane, personal communication, July 24, 2017).

In order to address these problems, new regions of interest were defined. To account for the number of data points, only 7-8 10mm spherical regions were defined for each network (Table 5 and Figure 2). The coordinates used to define the DMN spheres were adapted from a meta-analysis (Laird et al., 2009) and have been used in other investigations of the network (Fallon et al., 2016). The coordinates for the ECN and SN were adapted from a previous study which isolated both networks (Seeley et al., 2007) and were used in a recent study (Androulakis et al., 2017). Although it is expected that the time series from regions within the same network would be highly correlated, the correlations among the spherical ROIs were not as high as the modified Shirer ROIs which helped reduce the multicollinearity problem. This is likely because the spherical regions were more spatially separated than the modified Shirer ROIs. The GIMME

algorithm was able to successfully fit both group-level and individual-level connectivity maps using these new ROIs.

Table 5.

*Spherical Regions of Interest*

Region	Hemisphere	<i>x</i>	<i>y</i>	<i>z</i>
<b>Default Mode Network</b>				
Precuneus	Left	-4	-58	44
Posterior Cingulate	Left	-4	-52	22
Medial Prefrontal Cortex	Left	-2	50	18
Ventral Anterior Cingulate	Right	2	32	-8
Inferior Parietal Lobule	Right	52	-28	24
Inferior Parietal Lobule	Left	-56	-36	28
Middle Frontal Gyrus	Left	-26	16	44
<b>Executive Control Network</b>				
Dorsolateral Prefrontal Cortex	Left	-34	46	6
Dorsolateral Prefrontal Cortex	Right	46	46	14
Dorsomedial Prefrontal Cortex	-	0	36	46
Inferior Frontal Gyrus	Right	56	14	14
Ventromedial Caudate	Right	10	12	2
Lateral Parietal	Left	-48	-48	48
Lateral Parietal	Right	38	-56	44
<b>Salience Network</b>				
Dorsomedial Thalamus	Right	12	-18	6
Dorsal Anterior Cingulate	Left	-6	18	30
Orbital Frontal Insula	Left	-40	18	-12
Orbital Frontal Insula	Right	42	10	-12
Substantia Nigra/	Left	-10	-14	-10
Ventral Tegmental Area				
Substantia Nigra/	Right	8	-8	-14
Ventral Tegmental Area				
Ventral Striatum/Pallidum	Left	-22	12	-6
Ventral Striatum/Pallidum	Right	22	6	-2

*Note:* *x*, *y*, and *z* correspond to the MNI coordinates used to generate each region.



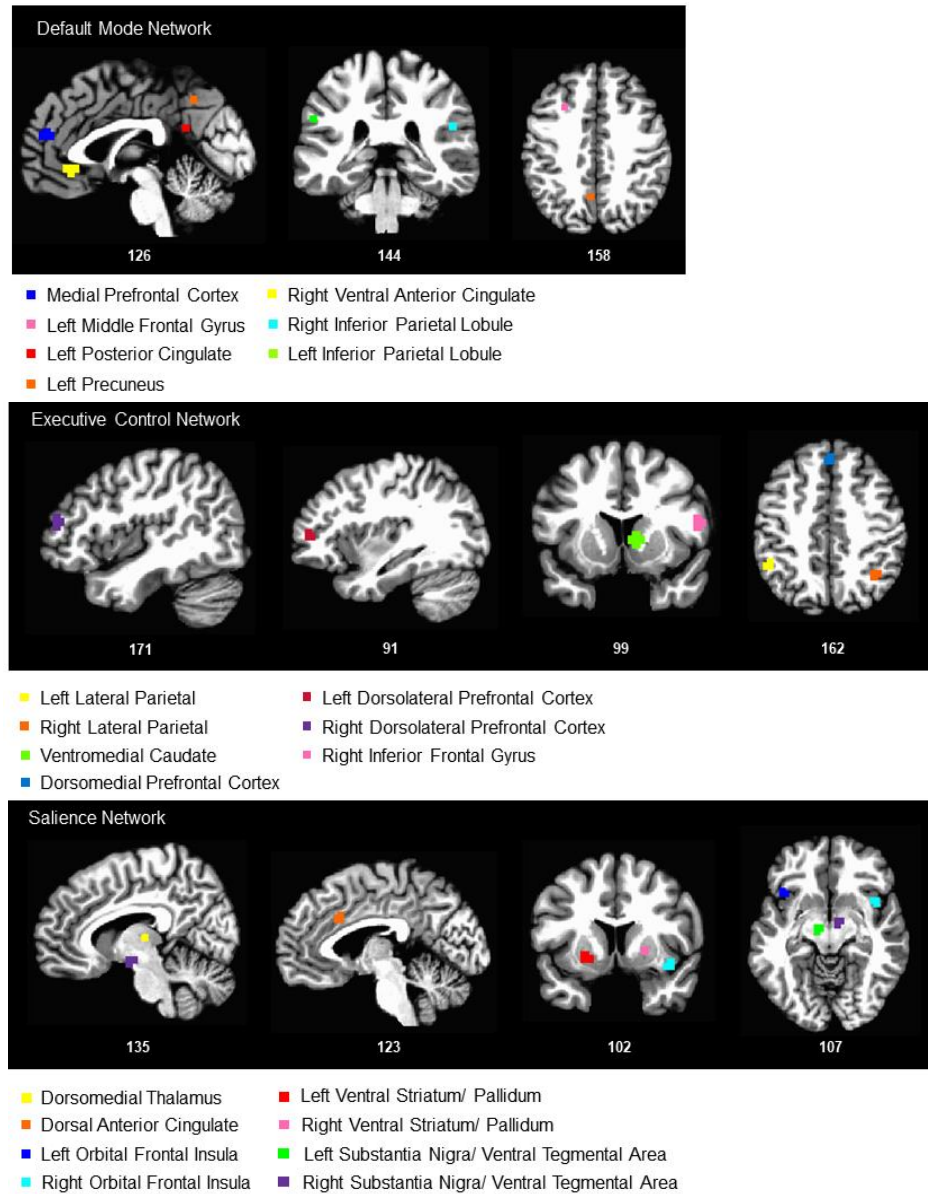


Figure 2. Spherical Regions of Interest

### Fit Parameters

In order to test whether the results obtained after running the GIMME algorithm were stable, a number of default parameters were modified. The first parameter that was modified was the group-level cut-off which by default is set at .75 indicating that at least

75% of the participants have connectivity maps with good model fit as indexed by standard SEM fit indices (e.g. root mean square error of approximation, RMSEA < .05; standardized root meansquare residual, SRMR < .05; non-normed fit index, NNFI > .95; comparative fit index, CFI > .95). A similar parameter that was modified was the subgroup-level cut-off which by default is set at .50 indicating that at least 50% of the subgroup is well described by the subgroup-level connectivity map as indexed by the standard SEM fit indices. These parameters were modified such that the algorithm examined the combination of the group-level cut-off set at .70, .75, and .80 and the subgroup level cut-off set at .50 and .55 resulting in a total of 6 results for each network.

### Independent Component Analysis

Independent component analysis was run on the final preprocessed functional images in the Group ICA of fMRI Toolbox (ICA GIFT v4.0a) to establish networks of spatially distinct, temporally correlated regions (Calhoun et al., 2004; Calhoun, Adali, Pearlson, & Pekar, 2001). Two separate ICAs were run. The first ICA was run on the matched sample, and the second ICA on the full sample of participants. In each ICA, the data were reduced through single-subject principle component analysis (PCA) with temporal concatenation and group level PCA. The number of independent components within the data were freely estimated using minimum descriptive length (MDL) criteria. There was variability in the number of estimated components across individual participants, but 25 components were estimated for both the matched and full sample of participants. Spatial ICA with Infomax was run on this reduced data and independent spatial component maps were constructed for the group as well as each subject. A stability analysis was run using

ICASSO to estimate the reliability of the components over 10 iterations of this ICA algorithm. After visual inspection of the resulting components, artefactual (matched sample:  $n = 5$ ; full sample:  $n = 4$ ) and unstable components (matched sample:  $n = 0$ ; full sample:  $n = 1$ ) were eliminated from the dataset. This resulted in a final set of independent components for each task. A Monte Carlo simulation was run on the average component mask using 3dClustSim in AFNI and yielded a threshold of 31 and 43 contiguous voxels for the matched and full samples respectively at an uncorrected  $p$  value of .001 (FWE = .05). These voxel thresholds were used to define the group-level component masks prior to creating the binarized mask.

The 20 identified group-level components were used as masks to investigate variation from the group average at the individual level. A number of values were extracted from the voxels falling within the masked region in the individual-level component maps: 1) the average z-score, 2) the average positively thresholded ( $> 0$ ) z-score, and 3) the total count of the positively thresholded ( $> 0$ ) z-scores. The count of the average positively thresholded voxels was highly consistent across participants ( $r > .90$ ), and was thus not used as the basis for the clustering algorithm. The z-scores in the individual component maps indicate the contribution of individual voxels to that component. Thus, a higher z-score reflects a greater contribution to the component, and a positive score indicates that the voxel is positively correlated with the component (e.g. is not anti-correlated).

## Community Detection Analysis

The z-scores extracted from the individual component maps were configured into a participant by z-score matrix which was used for the community detection analysis which was implemented in R. Briefly, the algorithm calculates a correlation matrix and sets the diagonal of this matrix to 0 to avoid generating an adjacency matrix with looped connections. An adjacency matrix is then created by applying a threshold to the correlation matrix such that a “1” indicates a connection between participants and a “0” indicates no connection. The threshold was set to ensure that no participant had no connections (e.g. every participant had to have at least one connection in the adjacency matrix). Additionally, to ensure that the results were stable and not overly sensitive to minor fluctuations in the threshold, the algorithm was run at varied thresholds. After establishing these connections, the edge betweenness was calculated for each edge, and the edges with the highest betweenness centrality were removed until no more edges remained in the network and the community structure was identified.

The community detection analysis was run on both the matched sample and the full sample of participants. The analysis was run using the mean z-scores and the mean positively thresholded z-scores for the matched sample group and only the mean z-scores for the full sample group.

## CHAPTER THREE

### RESULTS

#### Overview

The results of both the GIMME analysis and the community detection analysis were limited due to the quality and length of data resulting in either no meaningful subgroups emerging from the data or in subgroups that were unstable and uninterpretable. The GIMME group-level connectivity maps varied across the tested thresholds and were sparse for each of the networks with no group-level connections arising in the DMN and ECN. The subgroup connectivity maps for each network were also threshold dependent suggesting that the identified subgroups were not robust. For the community detection analysis, one large cluster was identified which contained the majority of participants. The remaining participants were classified as outliers. This same pattern of results was seen when the community detection algorithm was run using the larger, more heterogeneous sample. Despite limitations inherent to the data, the results of the present study provide methodological pipelines which can be used to study highly heterogeneous datasets.

#### GIMME Analysis

Although the GIMME algorithm was able to arrive at group connectivity maps with adequate fit, the resulting maps were both unstable and weakly connected. The algorithm

favors the identification of a sparse group-level connectivity map with additional connections appearing at the subgroup level. However, in order to arrive at acceptable model fit, the algorithm removed all of the group-level paths among the ROIs. Additionally, for some of the networks, the group and subgroup results were not consistent across the varied thresholds. There were a number of subgroups identified that contained very few participants and many of these smaller subgroups were excluded after the subgroup-level cut-off was applied (e.g. .50 or .55). This resulted in several outlier participants who were not well described by the group or subgroup connectivity maps. The number of TD, ASD, and ADHD participants in subgroups derived across the modified parameters is presented in Table 6. For ease of reporting the results concisely, only the connections among the connectivity maps derived from the default threshold parameters (e.g. group threshold: .75, subgroup threshold: .50) will be discussed in depth, but all results across the modified thresholds are presented graphically (Figures 3-11). A comparison of the behavioral information for participants within the subgroups identified using the default parameters is presented in Figure 12.

#### *Default Mode Network*

For the DMN, no group level paths were identified, and this result was roughly consistent across the modified group-level thresholds (Figure 3). A total of 7 subgroups were identified, but, depending on the group threshold, 4-5 of these subgroups contained only 1 participant, and thus connectivity maps were not generated for these subgroups. When the group threshold was set at .70, the results differed from the results obtained at

the other group-level thresholds resulting in a divergence in the obtained connectivity maps and the number of subgroups.

There were two subgroups identified when using the default thresholds (Figures 6-7). The first subgroup which was comprised of 9 TD, 8 ASD, and 11 ADHD participants was characterized by connections from Left Posterior Cingulate Cortex to Left Middle Frontal Gyrus, Left Medial Prefrontal Cortex, and Left Precuneus. The second identified subgroup was comprised of 9 TD, 12 ASD, and 6 ADHD participants and was characterized by the following connections: Left Medial Prefrontal Cortex → Left Posterior Cingulate Cortex; Right Ventral Anterior Cingulate Cortex → Left Medial Prefrontal Cortex; Right Inferior Parietal Lobule → Left Inferior Parietal Lobule. There were a total of 5 outlier participants who were not included in either of the subgroups. Overall, there were no significant differences on the behavioral measures between the participants within the identified subgroups. The mean scores for the Inattentive and Hyperactive/Impulsive subscales were moderate (range: 59.94 to 66.56) as were the ADOS-2 scores. The mean scores on the SRS subscales indicated mild impairment for each subgroup (range: 57.64 to 65.27). Across both subgroups, mean scores on the ADI-R were high for the social (> 18), verbal (> 15) and RRB (> 5) subscales. Demographic information for the participants in the subgroups identified using the default group and subgroup threshold are displayed in Table 7.

#### *Executive Control Network*

Across all of the modified group-level thresholds, no group-level paths were identified among the ECN regions (Figure 4). The results were highly consistent across

the group-level results and the subgroup-level results. A total of 8 subgroups were identified, but 6 of these subgroups contained only 1 participant and connectivity maps were not generated resulting in 2 robust subgroups (Figures 8-9). The same participants were represented in the subgroups across the modified parameters and the connectivity maps were relatively consistent with minor differences seen at the more conservative subgroup threshold of .55.

In the first subgroup, there were 8 TD, 12 ASD, and 15 ADHD participants who were characterized by two connections: Right Ventromedial Caudate → Dorsomedial Prefrontal Cortex and Left Lateral Parietal → Right Lateral Parietal. A total of 9 TD, 6 ASD, and 4 ADHD participants were included in the second subgroup which was defined by two connections: Left Lateral Parietal → Left Dorsolateral Prefrontal Cortex and Right Dorsolateral Prefrontal Cortex → Right Inferior Frontal Gyrus. There were 6 outlier participants who were not included in either of the subgroups. Overall, there were no significant differences on the behavioral measures between the participants within the identified subgroups. The mean scores for the Inattentive and Hyperactive/Impulsive subscales were mild (< 63). The ADOS-2 scores were moderate across both subgroups. The mean scores on the SRS subscales indicated mild to moderate impairment for each subgroup (range: 53.83 to 76.36). Across both subgroups, mean scores on the ADI-R were high for the social (> 17), verbal (> 15) and RRB (> 4) subscales. Demographic information for the participants in the subgroups identified using the default group and subgroup threshold are displayed in Table 8.



### *Salience Network*

Modification of the group-level thresholds resulted in instability in SN results (Figure 5). At a group-level threshold of .70, the SN had one connection from the Right Ventral Striatum/ Pallidum to the Left Ventral Striatum/ Pallidum but this connection was not seen at the other thresholds. Similar to the DMN results, connectivity maps generated at a group-level threshold of .70 were roughly consistent across the modified subgroup parameters, but these results were dissimilar from the connectivity maps obtained at the other group-level thresholds. A total of 9 subgroups were identified, but 6 of these subgroups contained only 1 participant and thus connectivity maps were not generated for these subgroups.

With the default parameters, a total of three subgroups were identified (Figures 10-11). The first subgroup was comprised of 12 TD, 14 ASD, and 11 ADHD participants and was characterized by connections from the Right Ventral Striatum/ Pallidum to Left Ventral Striatum/ Pallidum, Right Dorsomedial Thalamus, and Left Dorsal Anterior Cingulate Cortex. The second subgroup had 4 TD, 4 ASD, and 7 ADHD participants and had the following connections: Left Substantia Nigra/ Ventral Tegmental Area → Left Orbital Frontal Insula, Right Dorsomedial Thalamus, and Right Substantia Nigra/ Ventral Tegmental Area; Right Dorsomedial Thalamus → Right Ventral Striatum/ Pallidum and Left Dorsal Anterior Cingulate; Left Orbital Frontal Insula → Right Orbital Frontal Insula; Right Ventral Striatum/ Pallidum → Left Ventral Striatum/ Pallidum and Left Dorsal Anterior Cingulate. The third subgroup only had 2 TD participants who had the following connections: Left Substantia Nigra/ Ventral Tegmental Area → Right Dorsomedial Thalamus and Right Substantia Nigra/ Ventral Tegmental Area; Left Orbital

Frontal Insula  $\leftrightarrow$  Right Ventral Striatum/ Pallidum; Right Dorsomedial Thalamus  $\rightarrow$  Right Ventral Striatum/ Pallidum; Right Ventral Striatum/ Pallidum  $\rightarrow$  Left Ventral Striatum/ Pallidum and Left Dorsal Anterior Cingulate; Left Dorsal Anterior Cingulate  $\rightarrow$  Left Ventral Striatum/ Pallidum. There were 6 outlier participants who were not included in any of the three subgroups. Overall, there were no significant differences on the behavioral measures between the participants within the identified subgroups. The mean scores for the Inattentive and Hyperactive/Impulsive subscales were mild to moderate (range: 60.18 to 66.44). The ADOS-2 scores were mild to moderate across both subgroups. The mean scores on the SRS subscales indicated mild to moderate impairment for each subgroup (range: 59.00 to 71.50). For subgroup 1, the mean ADI-R scores were high for the social (20.43), verbal (17.21), and RRB (5.79) subscales. For subgroup 2, the mean ADI-R scores were also high but slightly lower than the subgroup 1 for the social (11.75), verbal (12.75), and RRB (6.25) subscales. Demographic information for the participants in the subgroups identified using the default group and subgroup threshold are displayed in Table 9.

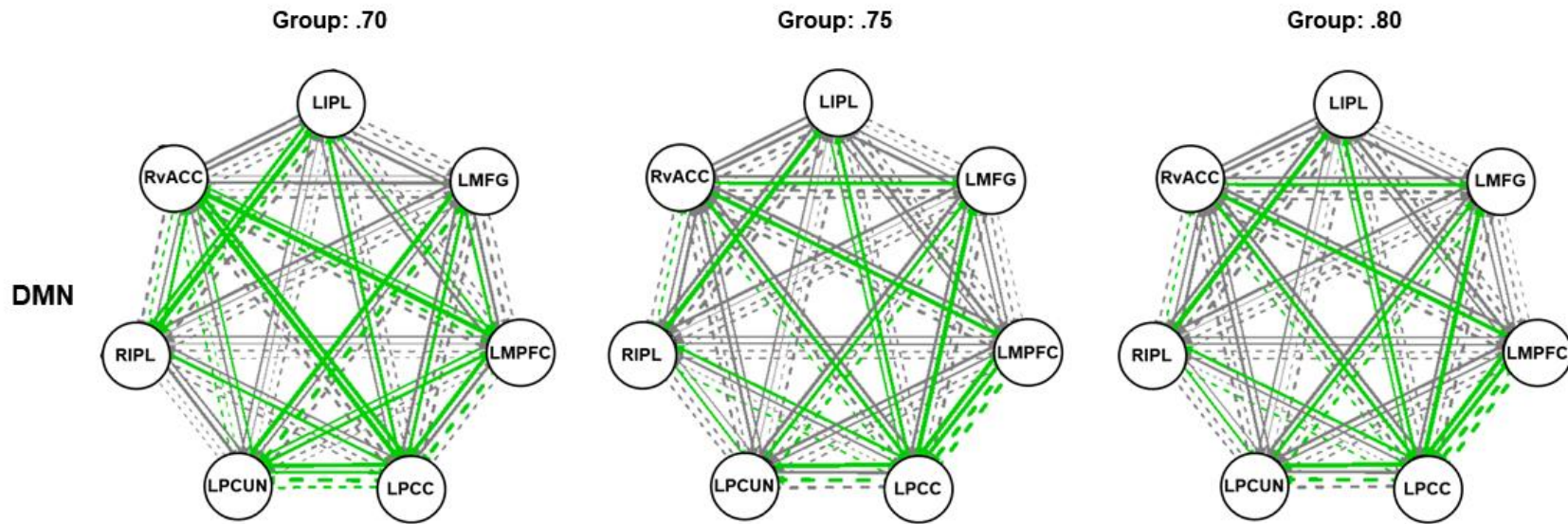


*Figure 3.* Group Connectivity Maps for the Default Mode Network. Results are shown across group-level thresholds: .70 (left), .75 (middle), .80 (right). Group level paths are shown in black, subgroup level paths are shown in green, and individual level paths are shown in grey. The line thickness corresponds to the number of individuals with a connection. Contemporaneous connections are depicted with solid lines, and lagged connections are depicted with dashed lines. LIPL = Left Inferior Parietal Lobule; LMFG = Left Middle Frontal Gyrus; LMPFC = Left Medial Prefrontal Cortex; LPCC = Left Posterior Cingulate Cortex; LPCUN = Left Precuneus; RIPL = Right Inferior Parietal Lobule; RvACC = Right Ventral Anterior Cingulate Cortex.

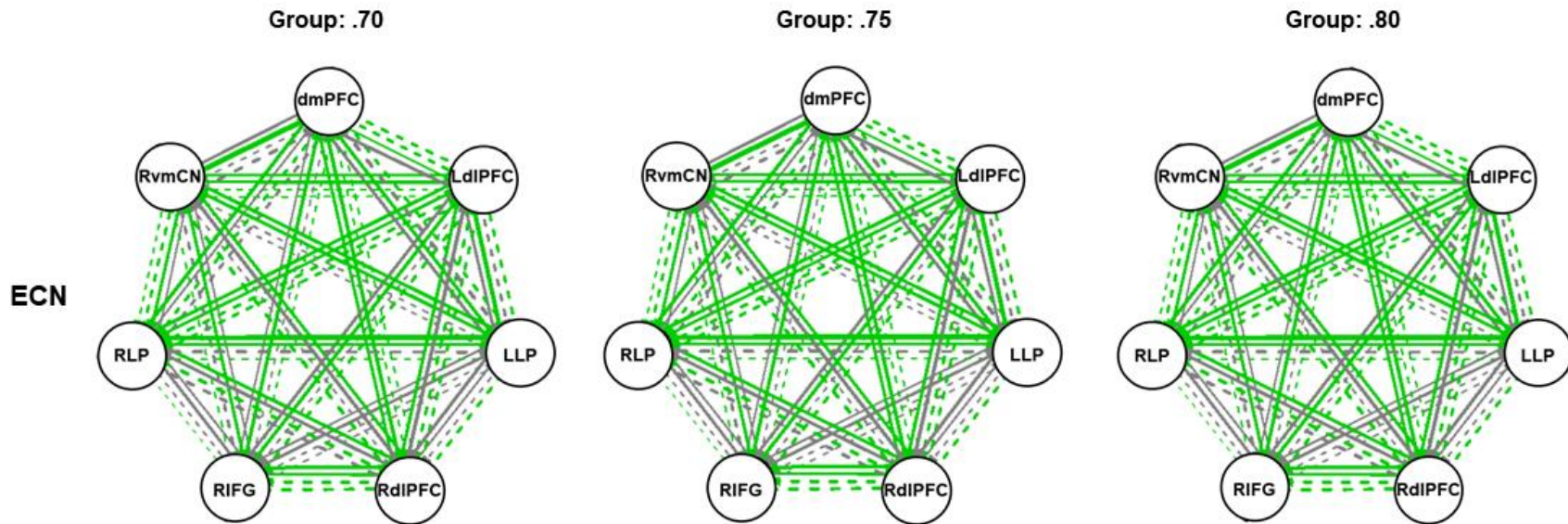


*Figure 4.* Group Connectivity Maps for the Executive Control Network. Results are shown across group-level thresholds: .70 (left), .75 (middle), .80 (right). Group level paths are shown in black, subgroup level paths are shown in green, and individual level paths are shown in grey. The line thickness corresponds to the number of individuals with a connection. Contemporaneous connections are depicted with solid lines, and lagged connections are depicted with dashed lines. dmPFC = Dorsomedial Prefrontal Cortex; LdlPFC = Left Dorsolateral Prefrontal Cortex; LLP = Left Lateral Parietal; RdIPFC = Right Dorsolateral Prefrontal Cortex; RIFG = Right Inferior Frontal Gyrus; RLP = Right Lateral Parietal; RvmCN = Right Ventromedial Caudate Nucleus.

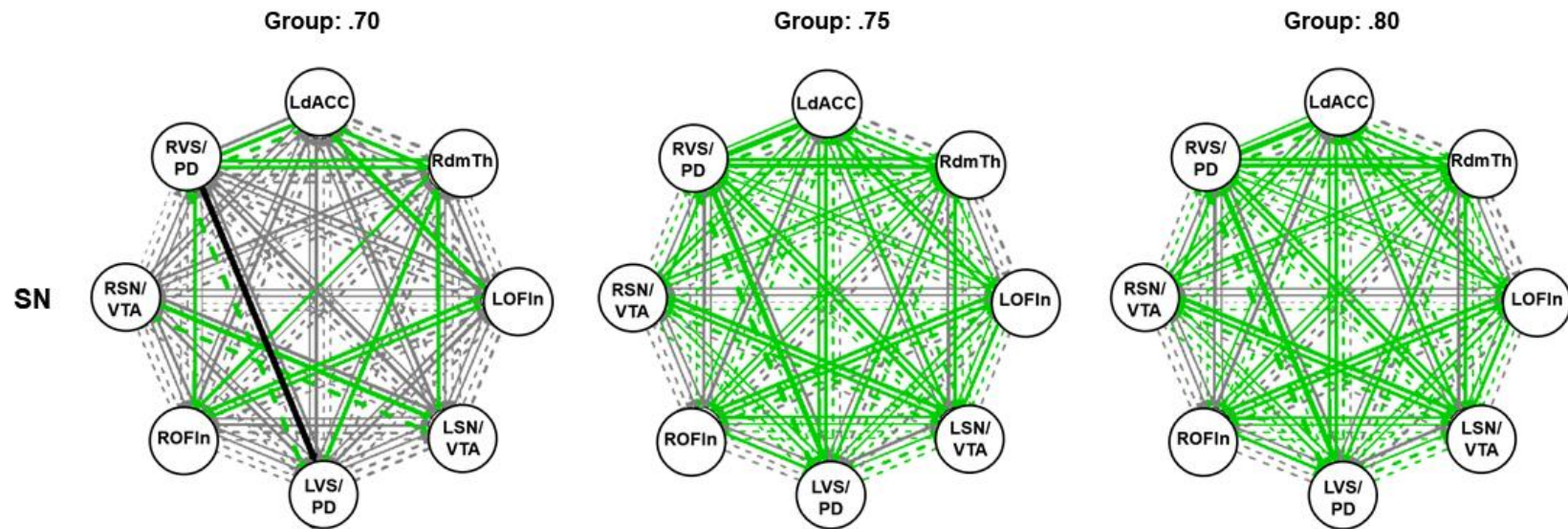


*Figure 5.* Group Connectivity Maps for the Salience Network. Results are shown across group-level thresholds: .70 (left), .75 (middle), .80 (right). Group level paths are shown in black, subgroup level paths are shown in green, and individual level paths are shown in grey. The line thickness corresponds to the number of individuals with a connection. Contemporaneous connections are depicted with solid lines, and lagged connections are depicted with dashed lines. LdACC = Left Dorsal Anterior Cingulate Cortex; RdmTh = Right Dorsomedial Thalamus; LOFIn = Left Orbital Frontal Insula; LSN/VTA = Left Substantia Nigra/ Ventral Tegmental Area; LVS/PD = Left Ventral Striatum/ Pallidum; ROFIn = Right Orbital Frontal Insula; RSN/VTA = Right Substantia Nigra/ Ventral Tegmental Area; RVS/PD = Right Ventral Striatum/ Pallidum.



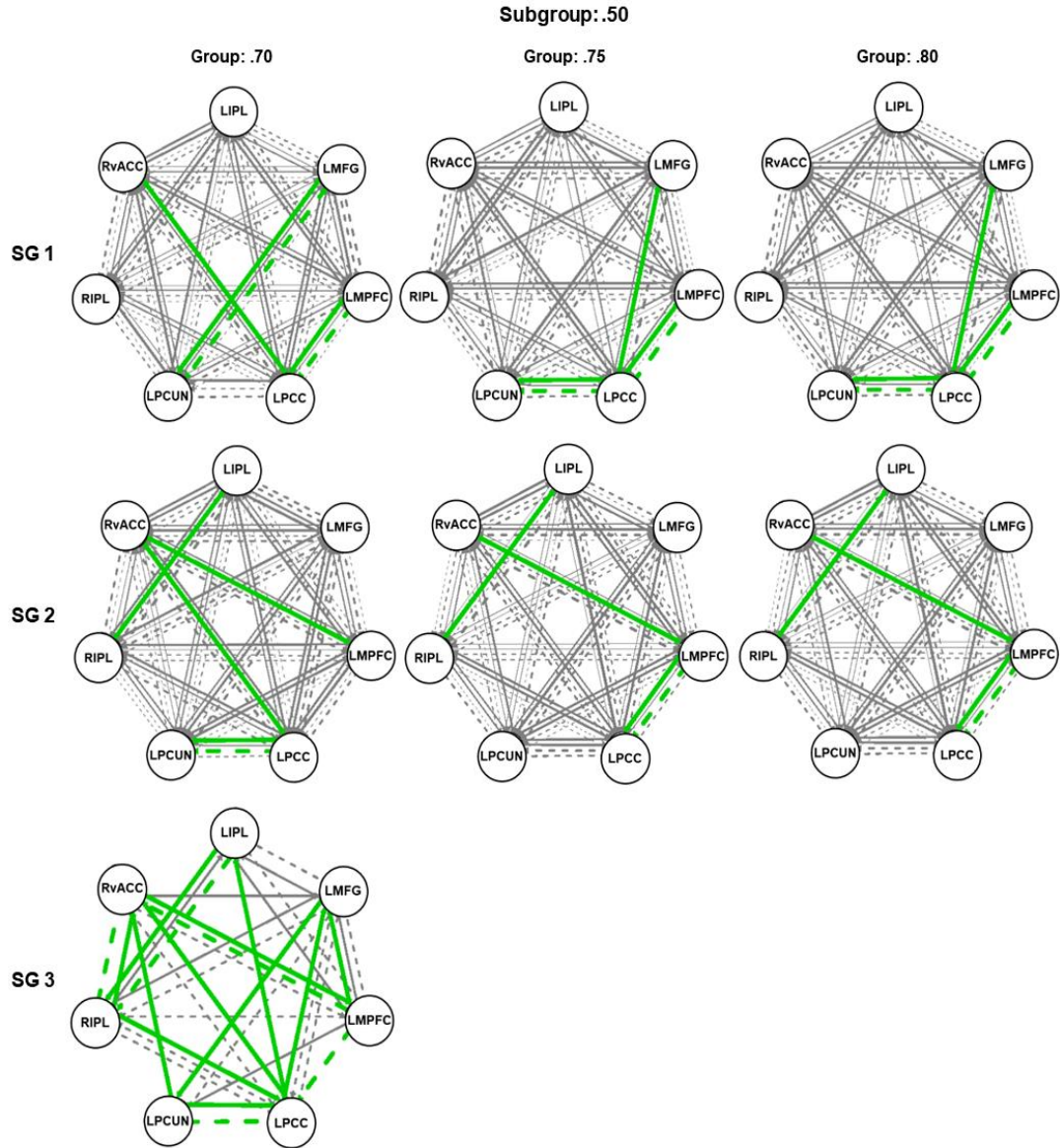


*Figure 6.* Subgroup Connectivity Maps for the Default Mode Network (.50 threshold). Results are shown across group-level thresholds: .70 (left), .75 (middle), .80 (right). Subgroup level paths are shown in green, and individual level paths are shown in grey. The line thickness corresponds to the number of individuals with a connection. Contemporaneous connections are depicted with solid lines, and lagged connections are depicted with dashed lines. LIPL = Left Inferior Parietal Lobule; LMFG = Left Middle Frontal Gyrus; LMPFC = Left Medial Prefrontal Cortex; LPCC = Left Posterior Cingulate Cortex; LPCUN = Left Precuneus; RIPL = Right Inferior Parietal Lobule; RvACC = Right Ventral Anterior Cingulate Cortex.

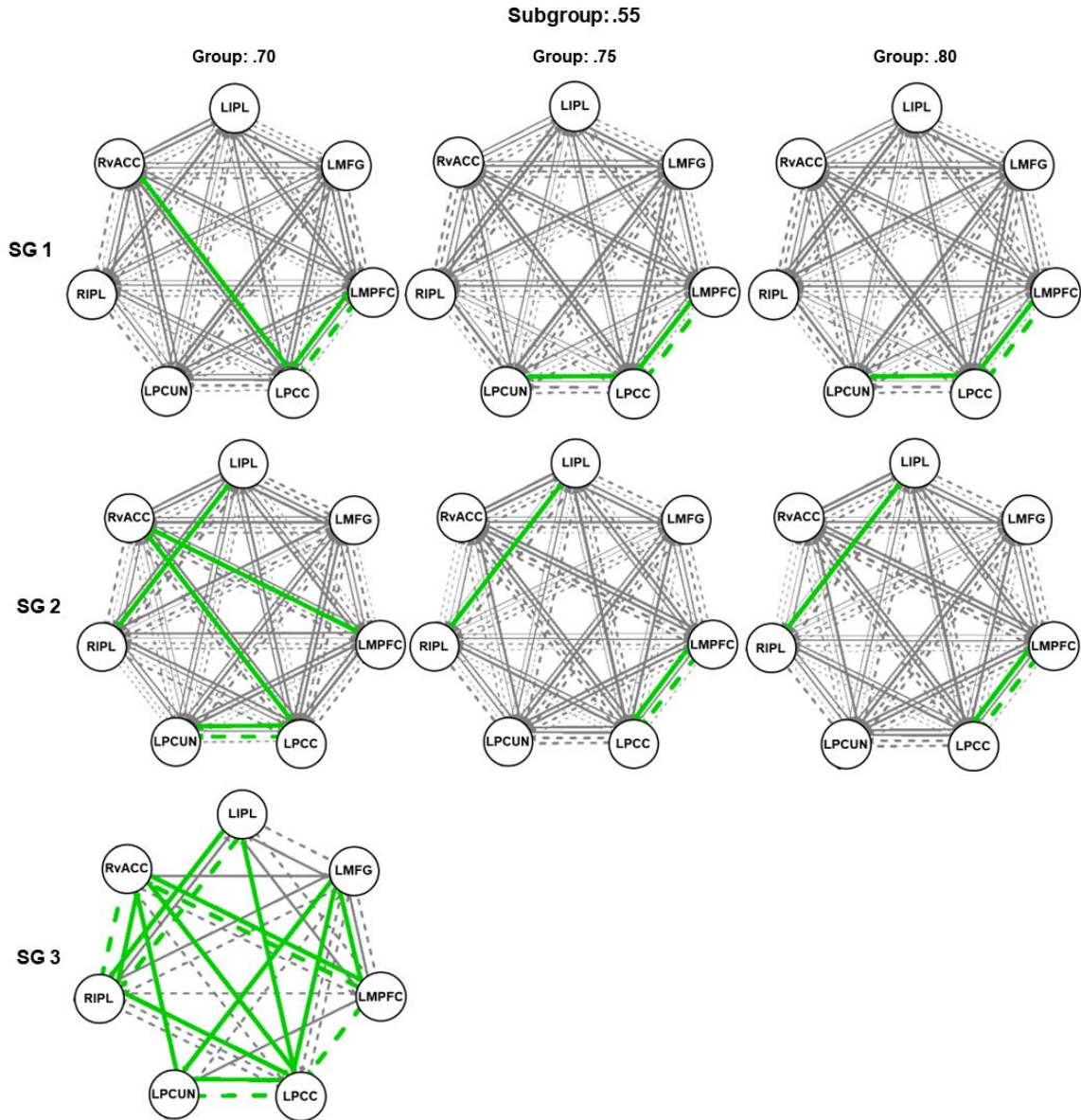


*Figure 7. Subgroup Connectivity Maps for the Default Mode Network (.55 threshold). Results are shown across group-level thresholds: .70 (left), .75 (middle), .80 (right). Subgroup level paths are shown in green, and individual level paths are shown in grey. The line thickness corresponds to the number of individuals with a connection. Contemporaneous connections are depicted with solid lines, and lagged connections are depicted with dashed lines. LIPL = Left Inferior Parietal Lobule; LMFG = Left Middle Frontal Gyrus; LMPFC = Left Medial Prefrontal Cortex; LPCC = Left Posterior Cingulate Cortex; LPCUN = Left Precuneus; RIPL = Right Inferior Parietal Lobule; RvACC = Right Ventral Anterior Cingulate Cortex.*

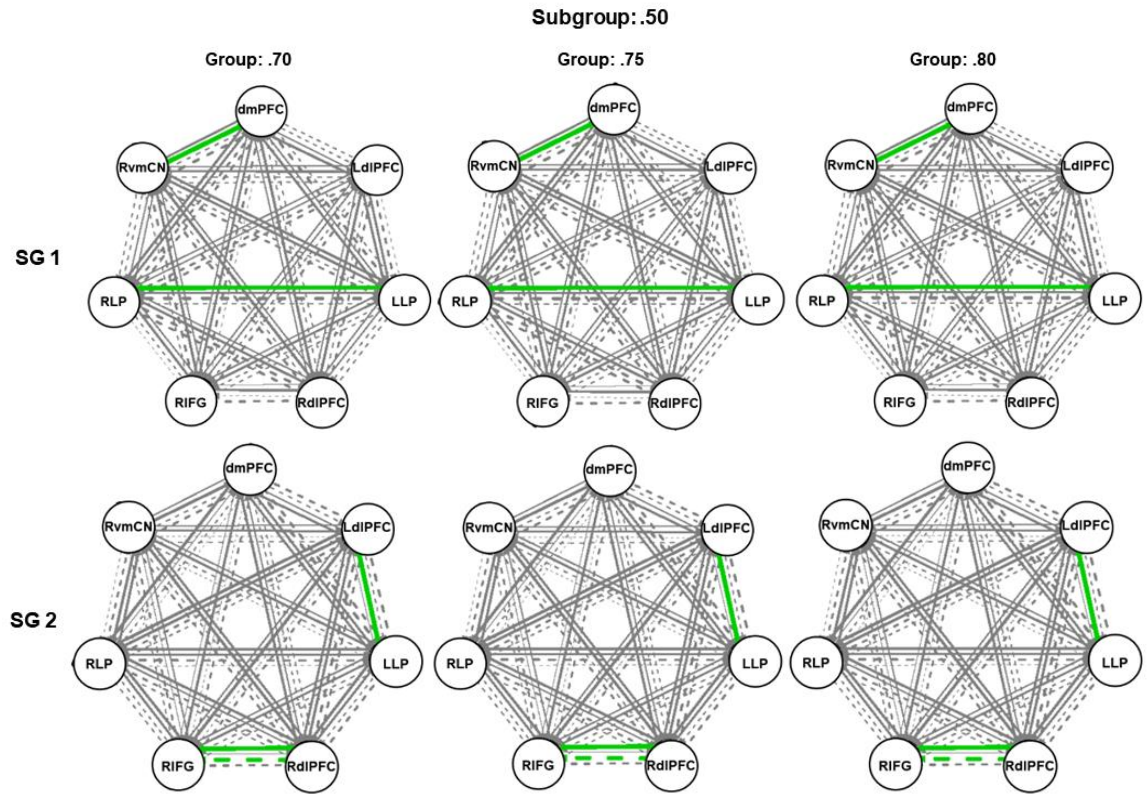


*Figure 8.* Subgroup Connectivity Maps for the Executive Control Network (.50 threshold). Results are shown across group-level thresholds: .70 (left), .75 (middle), .80 (right). Subgroup level paths are shown in green, and individual level paths are shown in grey. The line thickness corresponds to the number of individuals with a connection. Contemporaneous connections are depicted with solid lines, and lagged connections are depicted with dashed lines. dmPFC = Dorsomedial Prefrontal Cortex; LdlPFC = Left Dorsolateral Prefrontal Cortex; LLP = Left Lateral Parietal; RdIPFC = Right Dorsolateral Prefrontal Cortex; RIFG = Right Inferior Frontal Gyrus; RLP = Right Lateral Parietal; RvmCN = Right Ventromedial Caudate Nucleus.



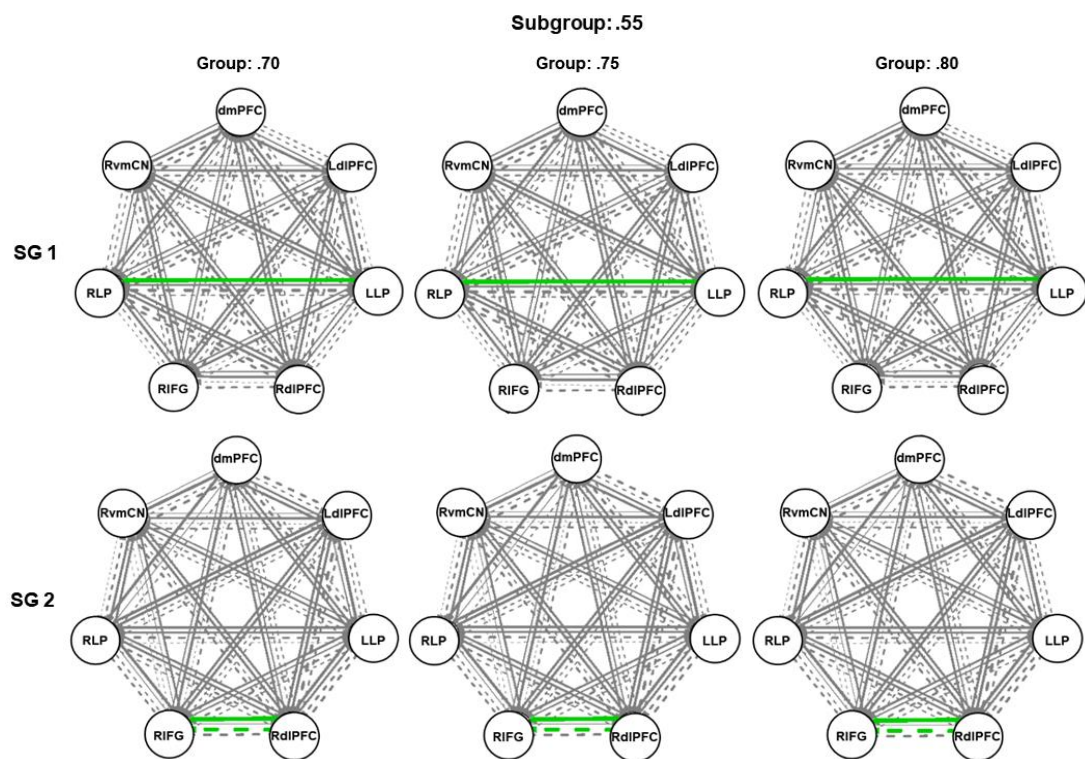


*Figure 9.* Subgroup Connectivity Maps for the Executive Control Network (.55 threshold). Results are shown across group-level thresholds: .70 (left), .75 (middle), .80 (right). Subgroup level paths are shown in green, and individual level paths are shown in grey. The line thickness corresponds to the number of individuals with a connection. Contemporaneous connections are depicted with solid lines, and lagged connections are depicted with dashed lines. dmPFC = Dorsomedial Prefrontal Cortex; LdlPFC = Left Dorsolateral Prefrontal Cortex; LLP = Left Lateral Parietal; RdIPFC = Right Dorsolateral Prefrontal Cortex; RIFG = Right Inferior Frontal Gyrus; RLP = Right Lateral Parietal; RvmCN = Right Ventromedial Caudate Nucleus.

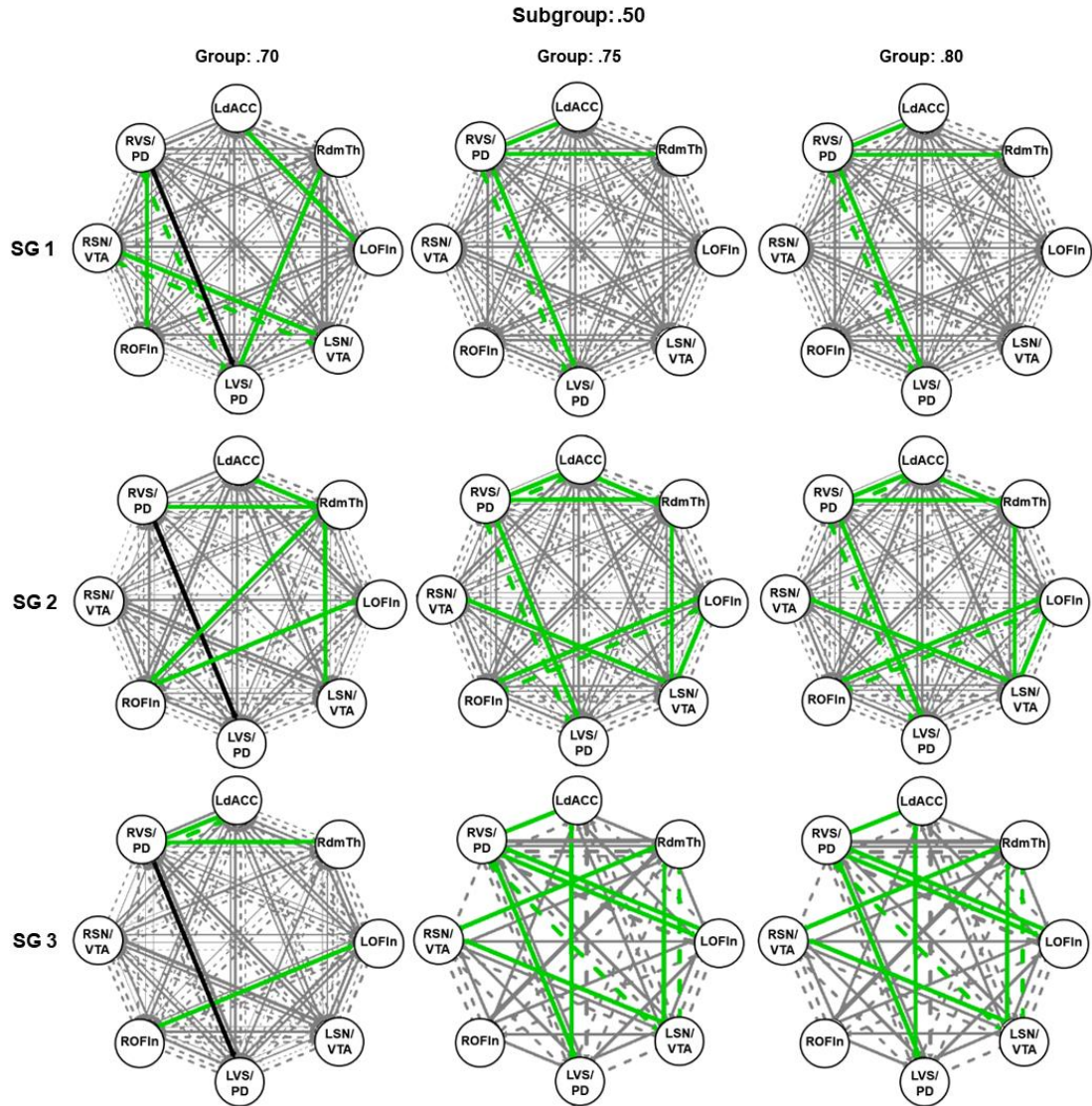


*Figure 10.* Subgroup Connectivity Maps for the Saliency Network (.50 threshold). Results are shown across group-level thresholds: .70 (left), .75 (middle), .80 (right). Group level paths are shown in black, subgroup level paths are shown in green, and individual level paths are shown in grey. The line thickness corresponds to the number of individuals with a connection. Contemporaneous connections are depicted with solid lines, and lagged connections are depicted with dashed lines. LdACC = Left Dorsal Anterior Cingulate Cortex; RdmTh = Right Dorsomedial Thalamus; LOFin = Left Orbital Frontal Insula; LSN/VTA = Left Substantia Nigra/ Ventral Tegmental Area; LVS/PD = Left Ventral Striatum/ Pallidum; ROFin = Right Orbital Frontal Insula; RSN/VTA = Right Substantia Nigra/ Ventral Tegmental Area; RVS/PD = Right Ventral Striatum/ Pallidum.

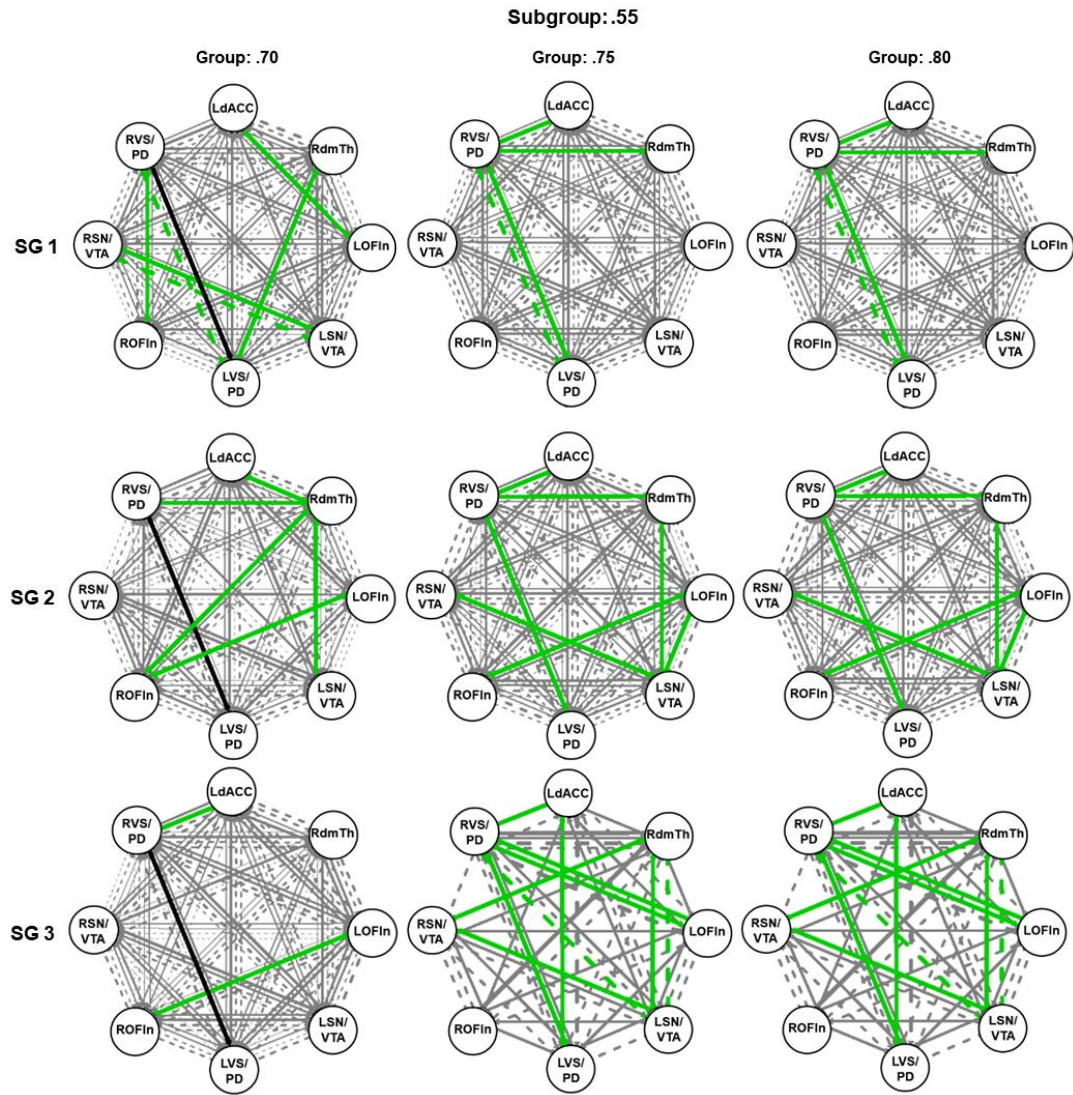


*Figure 11.* Subgroup Connectivity Maps for the Saliency Network (.55 threshold). Results are shown across group-level thresholds: .70 (left), .75 (middle), .80 (right). Group level paths are shown in black, subgroup level paths are shown in green, and individual level paths are shown in grey. The line thickness corresponds to the number of individuals with a connection. Contemporaneous connections are depicted with solid lines, and lagged connections are depicted with dashed lines. LdACC = Left Dorsal Anterior Cingulate Cortex; RdmTh = Right Dorsomedial Thalamus; LOFin = Left Orbital Frontal Insula; LSN/VTA = Left Substantia Nigra/ Ventral Tegmental Area; LVS/PD = Left Ventral Striatum/ Pallidum; ROFin = Right Orbital Frontal Insula; RSN/VTA = Right Substantia Nigra/ Ventral Tegmental Area; RVS/PD = Right Ventral Striatum/ Pallidum.



Table 6.

*Participant Subgroup Membership across Modified Thresholds*

Subgroup: .50										Subgroup: .55								
Group: .70			Group: .75			Group: .80				Group: .70			Group: .75			Group: .80		
DMN	1	2	3	1	2	3	1	2	3	1	2	3	1	2	3	1	2	3
SG 1	10	8	4	9	8	11	9	8	11	10	8	4	9	8	11	9	8	11
SG 2	9	9	15	9	12	6	9	12	6	9	9	15	9	12	6	9	12	6
SG 3		2	1	<b>1</b>			<b>1</b>				2	1	<b>1</b>			<b>1</b>		
SG 4		1		<b>1</b>			<b>1</b>				1		<b>1</b>			<b>1</b>		
SG 5	<b>1</b>					<b>1</b>			<b>1</b>	<b>1</b>					<b>1</b>			<b>1</b>
SG 6						<b>1</b>			<b>1</b>						<b>1</b>			<b>1</b>
SG 7						<b>1</b>			<b>1</b>						<b>1</b>			<b>1</b>
ECN	1	2	3	1	2	3	1	2	3	1	2	3	1	2	3	1	2	3
SG 1	8	12	15	8	12	15	8	12	15	8	12	15	8	12	15	8	12	15
SG 2	9	6	4	9	6	4	9	6	4	9	6	4	9	6	4	9	6	4
SG 3			<b>1</b>			<b>1</b>			<b>1</b>			<b>1</b>			<b>1</b>			<b>1</b>
SG 4		1			1			1			1			1			1	
SG 5	<b>1</b>			<b>1</b>			<b>1</b>			<b>1</b>			<b>1</b>			<b>1</b>		
SG 6	<b>1</b>			<b>1</b>			<b>1</b>			<b>1</b>			<b>1</b>			<b>1</b>		
SG 7		1			1			1			1			1			1	
SG 8	<b>1</b>			<b>1</b>			<b>1</b>			<b>1</b>			<b>1</b>			<b>1</b>		
SN	1	2	3	1	2	3	1	2	3	1	2	3	1	2	3	1	2	3
SG 1	9	6	14	12	14	11	12	14	11	9	6	14	12	14	11	12	14	11
SG 2	6	9	1	4	4	7	4	4	7	6	9	1	4	4	7	4	4	7
SG 3	5	5	5	2			2			5	5	5	2			2		
SG 4					<b>1</b>			<b>1</b>						<b>1</b>			<b>1</b>	
SG 5					<b>1</b>			<b>1</b>						<b>1</b>			<b>1</b>	
SG 6				<b>1</b>			<b>1</b>						<b>1</b>			<b>1</b>		
SG 7						<b>1</b>			<b>1</b>						<b>1</b>			<b>1</b>
SG 8				<b>1</b>			<b>1</b>						<b>1</b>			<b>1</b>		
SG 9						<b>1</b>			<b>1</b>						<b>1</b>			<b>1</b>

Note. Group 1 = TD, 2 = ASD, 3 = ADHD; SG = subgroup. Bolded numbers indicate outlier participants.

Table 7.

*Demographics for DMN Subgroups*

<b>Demographics</b>	<b>Subgroup 1</b>		<b>Subgroup 2</b>	
	N	Mean (SD)	N	Mean (SD)
TD	9	-	9	-
ASD	8	-	12	-
ADHD	11	-	6	-
M:F	21:7	-	22:6	-
Age	28	9.72 (1.65)	27	10.15 (1.57)
FIQ	28	112 (11.58)	27	108.44 (13.39)
<b>ADHD Measures</b>				
Inattentive	16	62.13 (11.74)	9	64.89 (15.71)
Hyper/Impulsive	16	59.94 (16.16)	9	66.56 (16.93)
<b>Autism Measures</b>				
ADI-R Social Total	8	18 (5.13)	12	18.75 (5.24)
ADI-R Verbal Total	8	16.25 (4.10)	12	15.58 (3.42)
ADI-R RRB Total	8	6.88 (2.03)	12	5 (2.09)
ADOS-2 Total	7	11.14 (1.57)	11	11.55 (3.47)
ADOS-2 Severity	7	6.57 (0.79)	11	6.33 (2.42)
ADOS-2 Social Affect	7	8 (1.41)	11	9 (3.38)
ADOS-2 RRB	7	3.14 (0.69)	11	2.55 (1.13)
SRS Total	11	63.27 (18.87)	17	63.71 (16.50)
SRS Social Awareness	11	65.27 (15.74)	17	62.59 (18.03)
SRS Social Cognition	11	57.64 (16.10)	17	59.53 (13.25)
SRS Social Communication	11	62.91 (18.05)	17	64.12 (17.10)
SRS Social Motivation	11	59.36 (16.75)	17	58.53 (13.03)
SRS Mannerisms	11	64.45 (19.41)	17	65.06 (16.51)

*Note:* The subgroups described here were identified using the default group threshold (.75) and subgroup threshold (.50). TD = Typically Developing; ASD = Autism Spectrum Disorder; ADHD = Attention Deficit Hyperactivity Disorder; M = Male; F = Female; FIQ = Full IQ Standard Score; ADI-R = Autism Diagnostic Interview-Revised; RRB = Restricted, Repetitive Behavior; ADOS = Autism Diagnostic Observation Schedule; SRS = Social Responsiveness Scale.

Table 8.

*Demographics for ECN Subgroups*

<b>Demographics</b>	<b>Subgroup 1</b>		<b>Subgroup 2</b>	
	N	Mean (SD)	N	Mean (SD)
TD	8	-	9	-
ASD	12	-	6	-
ADHD	15	-	4	-
M:F	24:9	-	16:5	-
Age	33	9.90 (1.77)	21	10.03 (1.33)
FIQ	33	111.48 (12.70)	21	111.57 (11.55)
<b>ADHD Measures</b>				
Inattentive	20	62.95 (13.71)	9	62.89 (14.29)
Hyper/Impulsive	20	62.15 (15.84)	9	62.89 (17.48)
<b>Autism Measures</b>				
ADI-R Social Total	12	17.67 (5.30)	6	19.00 (4.29)
ADI-R Verbal Total	12	15.92 (4.27)	6	15.50 (3.02)
ADI-R RRB Total	12	6.58 (2.15)	6	4.83 (1.72)
ADOS-2 Total	10	11.30 (2.26)	6	12.17 (3.87)
ADOS-2 Severity	11	6.09 (2.21)	6	7.17 (1.60)
ADOS-2 Social Affect	10	8.50 (2.42)	6	9.17 (3.82)
ADOS-2 RRB	10	2.80 (1.14)	6	3.00 (0.63)
SRS Total	11	74.00 (10.28)	12	58.33 (17.26)
SRS Social Awareness	11	72.00 (12.28)	12	61.25 (18.14)
SRS Social Cognition	11	68.82 (8.74)	12	53.83 (13.72)
SRS Social Communication	11	72.73 (9.76)	12	58.91 (17.66)
SRS Social Motivation	11	66.09 (11.48)	12	55.67 (14.84)
SRS Mannerisms	11	76.36 (11.91)	12	57.92 (16.02)

*Note:* The subgroups described here were identified using the default group threshold (.75) and subgroup threshold (.50). TD = Typically Developing; ASD = Autism Spectrum Disorder; ADHD = Attention Deficit Hyperactivity Disorder; M = Male; F = Female; FIQ = Full IQ Standard Score; ADI-R = Autism Diagnostic Interview-Revised; RRB = Restricted, Repetitive Behavior; ADOS = Autism Diagnostic Observation Schedule; SRS = Social Responsiveness Scale.

Table 9.

*Demographics for SN Subgroups*

	<b>Subgroup 1</b>		<b>Subgroup 2</b>		<b>Subgroup 3</b>	
<b>Demographics</b>	N	Mean (SD)	N	Mean (SD)	N	Mean (SD)
TD	12	-	4	-	2	-
ASD	14	-	4	-	-	-
ADHD	11	-	7	-	-	-
M:F	28:9	-	10:5	-	1:1	-
Age	37	9.89 (1.63)	15	9.64 (1.52)	2	9.88 (2.65)
FIQ	37	109.27 (13.19)	15	111.60 (10.77)	2	102 (2.83)
<b>ADHD Measures</b>						
Inattentive	17	62.65 (12.59)	9	66.44 (14.47)	1	46 (-)
Hyper/Impulsive	17	60.18 (13.78)	9	65.89 (19.10)	1	53 (-)
<b>Autism Measures</b>						
ADI-R Social Total	14	20.43 (4.09)	4	11.75 (1.26)	-	-
ADI-R Verbal Total	14	17.21 (3.36)	4	12.75 (2.22)	-	-
ADI-R RRB Total	14	5.79 (2.39)	4	6.25 (2.22)	-	-
ADOS-2 Total	12	11.67 (3.26)	4	10.50 (1.00)	-	-
ADOS-2 Severity	12	6.38 (2.33)	4	6.25 (0.50)	-	-
ADOS-2 Social Affect	12	9.00 (3.13)	4	7.50 (1.00)	-	-
ADOS-2 RRB	12	2.67 (1.23)	4	3.00 (0.00)	-	-
SRS Total	18	64.72 (15.26)	6	68.00 (22.54)	1	39 (-)
SRS Social Awareness	18	63.06 (15.54)	6	71.50 (17.78)	1	38 (-)
SRS Social Cognition	18	59.39 (11.90)	6	63.33 (19.65)	1	39 (-)
SRS Social Communication	18	65.72 (15.79)	6	66.50 (21.46)	1	38 (-)
SRS Social Motivation	18	60.39 (13.50)	6	59.00 (18.93)	1	42 (-)
SRS Mannerisms	18	65.39 (15.27)	6	71.50 (23.86)	1	43 (-)

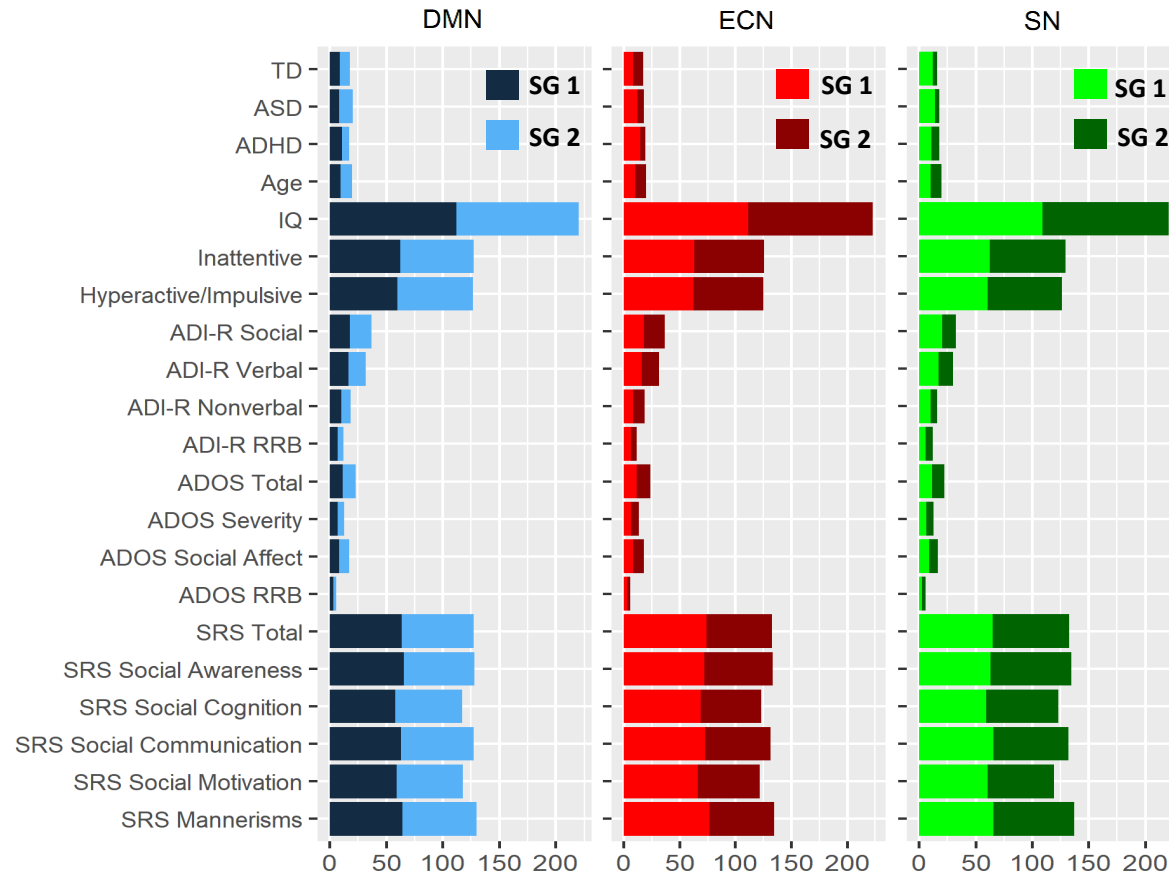


*Figure 12.* Behavioral Demographics across GIMME-Derived Subgroups. DMN = Default Mode Network; ECN = Executive Control Network; SN = Salience Network; SG = Subgroup; TD = Typically Developing; ASD = Autism Spectrum Disorder; ADHD = Attention Deficit Hyperactivity Disorder; M = Male; F = Female; ADI-R = Autism Diagnostic Interview-Revised; RRB = Restricted, Repetitive Behavior; ADOS = Autism Diagnostic Observation Schedule; SRS = Social Responsiveness Scale.



## ICA and Community Detection Analysis

The results of the community detection analysis for the matched sample are shown in Figure 13. The algorithm was run on the extracted mean z-scores and the positively thresholded z-scores from the matched sample group. Using the criteria that all participants had to have at least one connection, the thresholds applied to the correlation matrices for the mean z-score analysis ( $r = .58$ ) and the positively thresholded z-score analyses ( $r = .45$ ) differed slightly. With the exception of slight changes in the number of identified outlier participants, results were consistent across multiple thresholds. The results of both analyses were similar with one large cluster identified and several ( $n = 19 - 24$ ) outlier participants who were each clustered into their own individual group. All of the outlier participants for the mean z-score analysis and all but three of the participants for the positively thresholded z-score analyses were from the ADHD-200 database. The z-score analysis was repeated with the full sample of participants. The threshold applied to the correlation matrix was similar to the corresponding analysis with the matched sample ( $r = .59$ ). The result was consistent with the matched sample results (Figure 14), and, as expected, more outlier participants were detected in the larger sample ( $n = 49$ ). The average neuropsychological and behavioral battery scores for the primary matched sample cluster are presented in Table 10. The outlier participants from the mean z-score analysis using the matched group are characterized in Table 11.

Table 10.

*Demographics of Participants in Matched Sample Cluster*

<b>Demographics</b>	<b>N</b>	<b>Mean (SD)</b>
TD	13	-
ASD	20	-
ADHD	8	-
M:F	33:8	-
Age	41	10.22 (1.66)
FIQ	41	109.32 (13.16)
<b>ADHD Measures</b>		
Inattentive	11	62.91 (11.84)
Hyper/Impulsive	11	65.91 (15.81)
<b>Autism Measures</b>		
ADI-R Social Total	20	18.45 (5.07)
ADI-R Verbal Total	20	15.85 (3.62)
ADI-R RRB Total	20	5.75 (2.22)
ADOS-2 Total	18	11.39 (2.83)
ADOS-2 Severity	19	6.42 (1.95)
ADOS-2 Social Affect	18	8.61 (2.77)
ADOS-2 RRB	18	2.78 (1.00)
SRS Total	28	63.54 (17.12)
SRS Social Awareness	28	63.64 (16.92)
SRS Social Cognition	28	58.79 (14.17)
SRS Social Communication	28	63.64 (17.16)
SRS Social Motivation	28	58.86 (14.31)
SRS Mannerisms	28	64.82 (17.35)

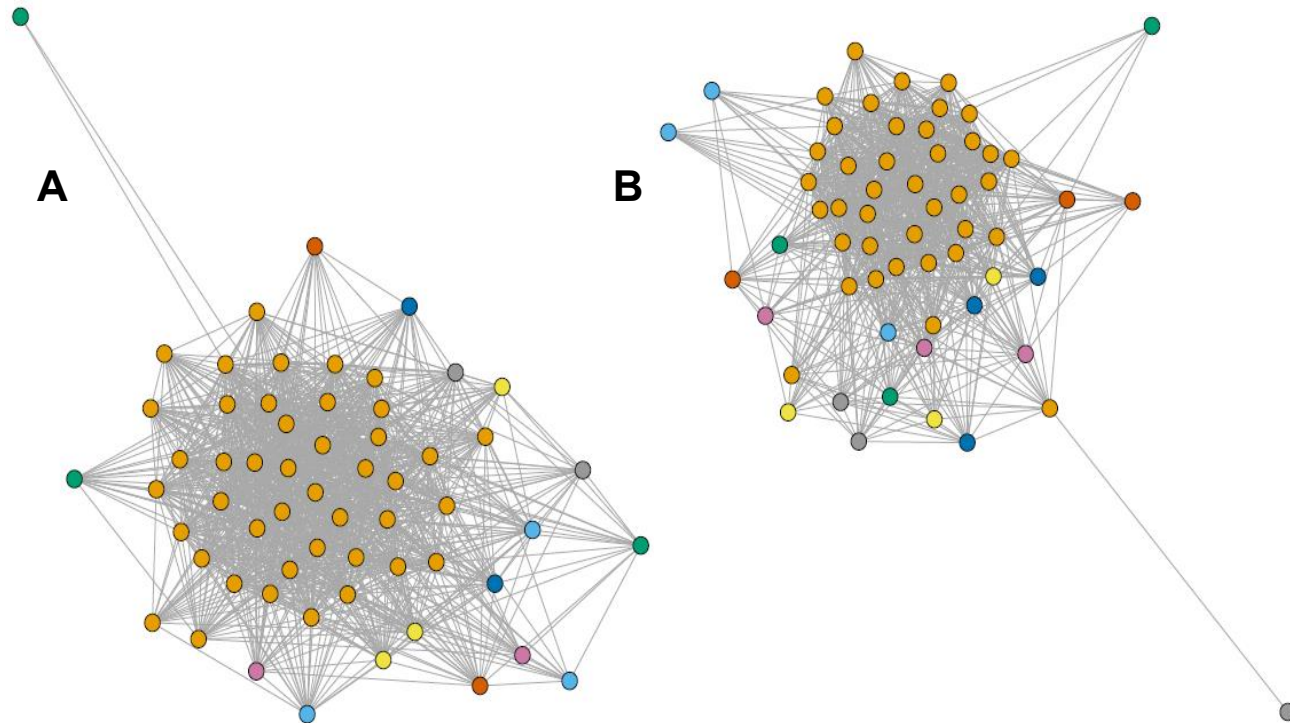
*Note:* M = Male; F = Female; FIQ = Full IQ Standard Score; ADI = Autism Diagnostic Interview-Revised; RRB = Restricted, Repetitive Behavior; ADOS = Autism Diagnostic Observation Schedule; SRS = Social Responsiveness Scale

Table 11.

*Outliers*

	1	2	3	4	5	6	7	8	9	10	11	12	13	14	15	16	17	18	19
Group	1	1	1	1	1	1	1	3	3	3	3	3	3	3	3	3	3	3	3
Age	9	11	8	11	8	8	8	11	8	7	9	8	8	9	8	8	8	9	9
Gender	F	M	M	M	M	F	M	M	M	F	F	M	M	M	F	M	F	M	F
FIQ	106	126	124	100	126	112	126	110	116	98	126	110	112	114	108	96	120	126	106
<b>ADHD</b>																			
In	48	40	55	46	41	56	43	69	70	80	69	63	70	67	90	63	79	70	79
H/Im	44	45	57	53	47	41	42	69	85	90	48	66	50	60	90	57	74	69	54

*Note.* Group: 1 = TD; 3 = ADHD; M = Male; F = Female; FIQ = Full IQ Standard Score; In = Inattentive Measure from the Conners' Rating Scale-3<sup>rd</sup> Edition; H/Im = Hyperactive/Impulsive Measure from the Conners' Rating Scale-3<sup>rd</sup> Edition



*Figure 13.* Community Detection Derived Clusters for Matched Sample. Results for the mean z-score analysis (**A**) and the positively thresholded mean z-score analysis (**B**) are shown. Each participant is represented with a circle. Circle color corresponds to assigned group membership. Dark orange circles represent participants assigned to the primary cluster.

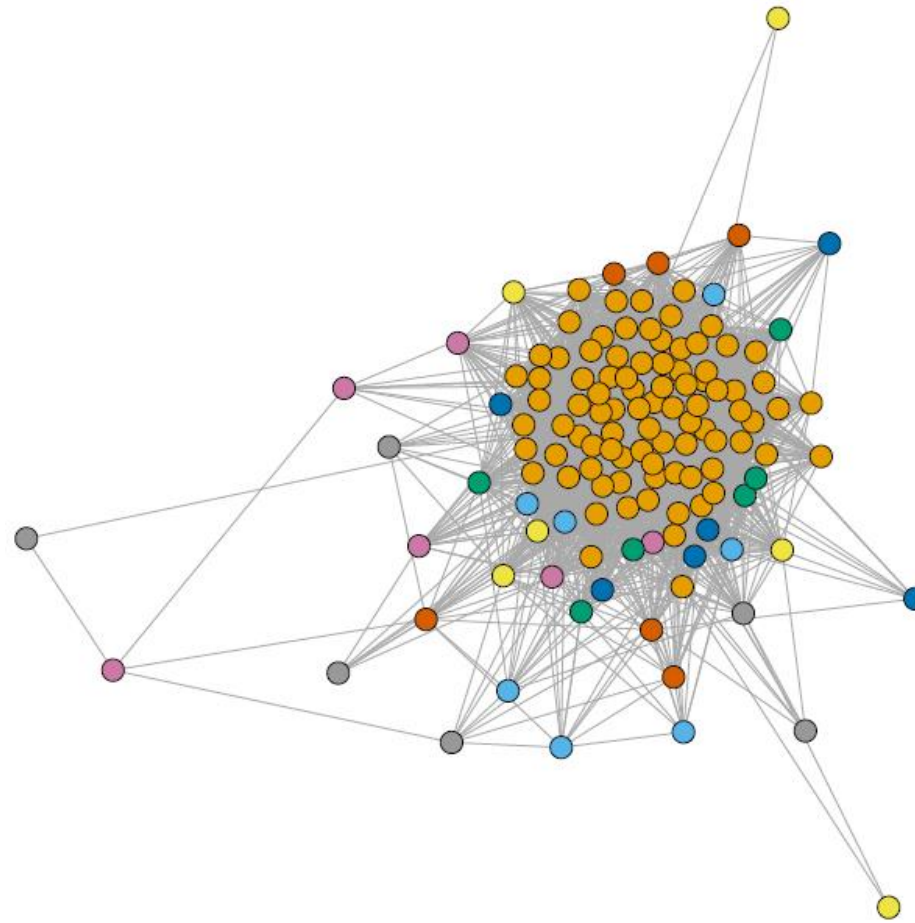


*Figure 14.* Community Detection Derived Cluster for Full Sample. Results for the mean z-score analysis are shown. Each participant is represented with a circle. Circle color corresponds to assigned group membership. Dark orange circles represent participants assigned to the primary cluster.

## CHAPTER FOUR

### DISCUSSION

This project was an attempt to address heterogeneity within neuroimaging data using complex mathematical models. The results of this study are broadly informative to researchers interested in applying mathematical models to study heterogeneity across different participant groups using resting-state fMRI data. Although the results of the GIMME algorithm and the ICA to community detection pipeline resulted in relatively unstable or null findings, these approaches provide a conceptual framework to model future investigations into heterogeneity across these participants groups. Specifically, the errors encountered in the GIMME analysis suggest that the data were insufficient and data with more time points may have provided a more robust result. The results of the ICA to community detection pipeline may also indicate an overall issue with the data or the methodological pipeline, but the lack of significant heterogeneity across the participants groups may also be a limitation.

Although the GIMME analysis of our dataset did not result in the findings we hypothesized, it is important to investigate the possible reasons for this outcome. The methodological issues encountered in this analysis limit the generalizability of the findings. Insufficient data resulted in an inability to use more than eight regions of interest, and using too few regions of interest resulted in unstable or uninterpretable results. This is primarily due to the lack of significant network connectivity seen at the

group level. It is possible that no group-level paths were identified due to the heterogeneity of the sample which resulted in the algorithm removing all paths, as the addition of any group-level paths did not adequately describe the majority of participants. The GIMME algorithm, however, is still a useful tool for researchers interested in investigating heterogeneity using resting-state data, task fMRI data, or behavioral data with a sufficient number of observations. The utility of this approach has been seen in recent research investigating olfactory networks (Karunanayaka et al., 2014), daily diary behavioral data (Lane & Gates, 2017), and resting-state data from depressed patients (Price et al., 2016), smokers (Zelle, Gates, Fiez, Sayette, & Wilson, 2016), and traumatic brain injury patients (Hillary, Medaglia, Gates, Molenaar, & Good, 2014).

Given the methodological limitations, the results of the GIMME analysis should be interpreted with caution. The GIMME analysis was run to piece apart individual differences in a highly heterogeneous sample; however, the groups were limited to equal sizes and roughly matched on age and IQ in order to avoid any inherent confounds between the groups. This is not an ideal solution as it severely restricts the variability within the sample and forces relative homogeneity on age and IQ which runs counter to the conceptual framework of this project. In addition, the connectivity maps generated by GIMME only include the set of regions identified prior to the analysis; therefore, ROI selection constrains the analysis and is an important consideration. The challenges regarding ROI selection may have, in part, impacted the outcome and the stability of the derived connectivity maps. Despite slight differences at the more liberal group-level threshold, the participants were consistently clustered into the same subgroups across the other group-level and subgroup-level thresholds. Additionally, with the exception of the

third SN subgroup, the subgroups were highly mixed with participants from each diagnostic group classified into all of the subgroups. This may suggest that heterogeneity exists at multiple levels: 1) within diagnostic groups as evidenced by the distribution of the participants from a given group across the subgroups; and 2) across diagnostic groups as evidenced by the mixture of participants from different groups within a single subgroup. It is known that individuals with ASD and ADHD display significant variability in cognition and behavior (Lenroot & Yeung, 2013; Wåhlstedt et al., 2009), but the results provided here may suggest that variability is also present across typical development. Theories of human development suggest that there are varied outcomes each within a typically developing group that are driven by contextual factors and genetic predispositions (Belsky & Pluess, 2009; Bronfenbrenner & Morris, 2007), but generally less attention is paid to individual variation in standard behavioral and neuroimaging studies.

The subgroups that were identified using the GIMME algorithm were characterized by mostly mild to moderate ADHD or ASD symptoms. Interestingly, a pattern of high scores for the ADI-R subscales was seen in conjunction with lower scores indicating less severity across the ADOS-2, SRS, and ADHD subscales of the CPRS-LV. Given the nature of neuroimaging studies which typically sample higher functioning individuals from clinical populations, it is expected that the behavioral scores would tend to reflect a mild or moderate symptom profile. The typically developing participants in the ABIDE-II database completed the SRS, but did not complete the ADI-R or the ADOS-2 thus the ADI-R scores are inflated in comparison to the other behavioral scores because they are derived from only participants with ASD who have higher scores. Conversely, the ADHD



subscales reported across all of the identified subgroups were completed by the ADHD and TD participants in the ADHD-200 database. Thus, the mild to moderate range of these scores reflects the fact that both TD and ADHD participants contribute to the average score.

In addition to the limitations inherent to the data, there are a number of potential problems that could have resulted in the community detection algorithm deriving one homogenous group. First, similar to the GIMME analysis, the data length may have been insufficient to capture the heterogeneity across the groups and the mathematical models may have been constrained by a lack of data. Second, the method itself may be flawed or may simply not be sensitive to detecting differences in network-level connectivity across participants groups. Both ICA and community detection have been used to study clinical populations, and the community detection algorithm used in the present study has been successfully used to subgroup participants with ADHD based on behavioral information (Fair et al., 2012; Karalunas et al., 2014). Despite the previous application of this algorithm to study ADHD in particular, a different community detection algorithm that does not rely on a small world principle with dense local connections and sparse long distance connections may prove more sensitive to detecting nuances in connectivity profiles. It is also possible that the community detection pipeline was overly sensitive to data quality which is highlighted by the finding that many of the outlier participants were from the ADHD-200 database which is older than the ABIDE-II database. Third, although the groups are from three distinct diagnostic groups, the heterogeneity among the participants is significantly limited considering only high functioning participants who can tolerate an hour-long scan session were included. Additionally, rigorous quality

assurance measures resulted in the removal of many of the ADHD participants and some of the ASD participants who had excessive motion during the scan. Matching participant groups also introduces an avenue where the participants become overly homogenous, but the same outcome was seen when the more heterogeneous full sample group was used. Fourth, the result may be a true finding suggesting that the groups do not differ in any coherent way in resting-state network connectivity. More likely, the groups may not differ systematically enough to identify patterns within network connectivity that are informative for clustering.

Although the analyses proposed here were largely stymied by methodological problems due to the amount and quality of the data, the primary goal of analyses of this nature should be to provide clinically meaningful information that can be used to better understand how variability across both clinical and typical populations impacts intervention, treatment, and developmental trajectories. There is a significant need to relate brain and behavior in a clinically meaningful way, and there is a corresponding need to understand how individual differences relate to both brain and behavior (Molenaar, 2015). Abnormalities in functional connectivity in each subgroup may relate to shared behavioral traits. Relating behavioral and diagnostic measures to the connectivity derived subgroups will allow for the study of TD participants who share common functional pathways with ASD or ADHD participants but fail to meet diagnostic criteria for the disorder. Finding altered connectivity in the absence of behavioral symptomatology consistent with a clinical disorder offers researchers and clinicians insight into any adaptive or compensatory mechanisms used by these participants which can serve to better future interventions. Additionally, studying how behaviors relate to

specific neural mechanisms can highlight whether subgroups exist in a given clinical disorder which is the first step in individualizing treatment. This information can also be used to predict response to treatment if a subgroup of a given disorder displays a pattern of functional connectivity that is markedly different from another subgroup comprised of individuals with the same clinical diagnosis. Thus, the focus of ongoing research should be in the individualized analysis of the interplay between brain and behavior in order to promote meaningful conclusions and personalized intervention planning.

## LIST OF REFERENCES

- Abbott, A. E., Nair, A., Keown, C. L., Datko, M., Jahedi, A., Fishman, I., & Müller, R.-A. (2016). Patterns of atypical functional connectivity and behavioral links in autism differ between default, salience, and executive networks. *Cerebral Cortex*, 26(10), 4034–4045. <http://doi.org/10.1093/cercor/bhv191>
- Amaral, L. A., Scala, A., Barthelemy, M., & Stanley, H. E. (2000). Classes of small-world networks. *Proceedings of the National Academy of Sciences of the United States of America*, 97(21), 11149–52. <http://doi.org/10.1073/pnas.200327197>
- American Psychiatric Association. (2013). *Diagnostic and statistical manual of mental disorders* (5th ed.). Arlington, VA: American Psychiatric Publishing.
- An, J. Y., & Claudianos, C. (2016). Genetic heterogeneity in autism: From single gene to a pathway perspective. *Neuroscience & Biobehavioral Reviews*, 68, 442–453. <http://doi.org/10.1016/j.neubiorev.2016.06.013>
- Andrews-Hanna, J. R., Smallwood, J., & Spreng, R. N. (2014). The default network and self-generated thought: Component processes, dynamic control, and clinical relevance. *Annals of the New York Academy of Sciences*, 1316, 29–52. <http://doi.org/10.1111/nyas.12360>
- Androulakis, X. M., Krebs, K., Peterlin, B. L., Zhang, T., Maleki, N., Sen, S., ... Herath, P. (2017). Modulation of intrinsic resting-state fMRI networks in women with

chronic migraine. *Neurology*, 89(2), 163–169.

<http://doi.org/10.1212/WNL.0000000000004089>

Assaf, M., Jagannathan, K., Calhoun, V. D., Miller, L., Stevens, M. C., Sahl, R., ...

Pearlson, G. D. (2010). Abnormal functional connectivity of default mode sub-networks in autism spectrum disorder patients. *NeuroImage*, 53(1), 247–256.

<http://doi.org/10.1016/j.neuroimage.2010.05.067>

Barabasi, A.-L., & Albert, R. (1999). Emergence of scaling in random networks.

<http://doi.org/10.1126/science.286.5439.509>

Belsky, J., & Pluess, M. (2009). The Nature (and Nurture?) of Plasticity in Early Human Development. *Perspectives on Psychological Science*, 4(4), 345–351.

<http://doi.org/10.1111/j.1745-6924.2009.01136.x>

Bentler, P. M., & Chou, C.-P. (1987). Practical issues in structural modeling.

*Sociological Methods & Research*, 16(1), 78–117.

<http://doi.org/10.1177/0049124187016001004>

Bigler, E. D., Mortensen, S., Neeley, E. S., Ozonoff, S., Krasny, L., Johnson, M., ...

Lainhart, J. E. (2007). Superior temporal gyrus, language function, and autism. *Developmental Neuropsychology*, 31(2), 217–238.

<http://doi.org/10.1080/87565640701190841>

Bishop, D. V. M., & Baird, G. (2001). Parent and teacher report of pragmatic aspects of communication: Use of the Children's Communication Checklist in a clinical setting. *Developmental Medicine and Child Neurology*, 43(12), 809.

<http://doi.org/10.1017/S0012162201001475>

- Brieber, S., Neufang, S., Bruning, N., Kamp-Becker, I., Remschmidt, H., Herpertz-Dahlmann, B., ... Konrad, K. (2007). Structural brain abnormalities in adolescents with autism spectrum disorder and patients with attention deficit/hyperactivity disorder. *Journal of Child Psychology and Psychiatry*, 48(12), 1251–1258.  
<http://doi.org/10.1111/j.1469-7610.2007.01799.x>
- Bronfenbrenner, U., & Morris, P. A. (2007). The Bioecological Model of Human Development. In *Handbook of Child Psychology*. Hoboken, NJ, USA: John Wiley & Sons, Inc. <http://doi.org/10.1002/9780470147658.chpsy0114>
- Bruining, H., de Sonnevile, L., Swaab, H., de Jonge, M., Kas, M., van Engeland, H., & Vorstman, J. (2010). Dissecting the clinical heterogeneity of autism spectrum disorders through defined genotypes. *PLoS ONE*, 5(5), e10887.  
<http://doi.org/10.1371/journal.pone.0010887>
- Calhoun, V. D., Pearlson, G., & Adali, T. (2004). Independent component analysis applied to fMRI Data : A generative model for validating results. *Signal Processing*, 281–291.
- Calhoun, Adali, T., Pearlson, G. D., & Pekar, J. J. (2001). A method for making group inferences from functional MRI data using independent component analysis. *Human Brain Mapping*, 14(3), 140–151. <http://doi.org/10.1002/hbm.1048>
- Castellanos, F. X., & Proal, E. (2012). Large-scale brain systems in ADHD: Beyond the prefrontal–striatal model. *Trends in Cognitive Sciences*, 16(1), 17–26.  
<http://doi.org/10.1016/j.tics.2011.11.007>
- Castellanos, F. X., Sonuga-Barke, E. J. S., Milham, M. P., & Tannock, R. (2006).

- Characterizing cognition in ADHD: Beyond executive dysfunction. *Trends in Cognitive Sciences*, 10(3), 117–123. <http://doi.org/10.1016/j.tics.2006.01.011>
- CDC. (2012). *Prevalence and Characteristics of Autism Spectrum Disorder Among Children Aged 8 Years — Autism and Developmental Disabilities Monitoring Network, 11 Sites, United States, 2012*.
- Conners, K. C. (1997). *Conners' Parent Rating Scale-Revised (L)*. North Tonawanda: Multi-Health Systems Inc.
- Constantino, J. N., & Gruber, C. P. (2012). *Social Responsiveness Scale, Second Edition (SRS-2)*. Torrance: CA: Western Psychological Services.
- Cox, R. W. (1996). AFNI: Software for analysis and visualization of functional magnetic resonance neuroimages. *Computers and Biomedical Research*, 29(3), 162–173. <http://doi.org/10.1006/cbmr.1996.0014>
- Dajani, D. R., Llabre, M. M., Nebel, M. B., Mostofsky, S. H., & Uddin, L. Q. (2016). Heterogeneity of executive functions among comorbid neurodevelopmental disorders. *Scientific Reports*, 6(1), 36566. <http://doi.org/10.1038/srep36566>
- Di Martino, A., Yan, C.-G., Li, Q., Denio, E., Castellanos, F. X., Alaerts, K., ... Milham, M. P. (2014). The autism brain imaging data exchange: Towards a large-scale evaluation of the intrinsic brain architecture in autism. *Molecular Psychiatry*, 19(6), 659–67. <http://doi.org/10.1038/mp.2013.78>
- Dichter, G. S. (2012). Functional magnetic resonance imaging of autism spectrum disorders. *Dialogues in Clinical Neuroscience*, 14(3), 319–51.

- Durston, S. (2008). Converging methods in studying attention-deficit/hyperactivity disorder: What can we learn from neuroimaging and genetics? *Development and Psychopathology*, 20(4), 1133. <http://doi.org/10.1017/S0954579408000539>
- Fair, D. A., Bathula, D., Nikolas, M. A., & Nigg, J. T. (2012). Distinct neuropsychological subgroups in typically developing youth inform heterogeneity in children with ADHD. *Proceedings of the National Academy of Sciences of the United States of America*, 109(17), 6769–74. <http://doi.org/10.1073/pnas.1115365109>
- Fallon, N., Chiu, Y., Nurmikko, T., Stancak, A., Nakamura, H., & Nishioka, K. (2016). Functional connectivity with the default mode network is altered in fibromyalgia patients. *PLOS ONE*, 11(7), e0159198. <http://doi.org/10.1371/journal.pone.0159198>
- Gargaro, B. A., Rinehart, N. J., Bradshaw, J. L., Tonge, B. J., & Sheppard, D. M. (2011). Autism and ADHD: How far have we come in the comorbidity debate? *Neuroscience and Biobehavioral Reviews*, 35(5), 1081–8. <http://doi.org/10.1016/j.neubiorev.2010.11.002>
- Gates, K. M., & Molenaar, P. C. M. (2012). Group search algorithm recovers effective connectivity maps for individuals in homogeneous and heterogeneous samples. *NeuroImage*, 63, 310–319. <http://doi.org/10.1016/j.neuroimage.2012.06.026>
- Gates, K. M., Molenaar, P. C. M., Hillary, F. G., Ram, N., & Rovine, M. J. (2010). Automatic search for fMRI connectivity mapping: An alternative to Granger causality testing using formal equivalences among SEM path modeling, VAR, and unified SEM. *NeuroImage*, 50(3), 1118–1125.



<http://doi.org/10.1016/j.neuroimage.2009.12.117>

Girvan, M., & Newman, M. E. J. (2002). Community structure in social and biological networks. *Proceedings of the National Academy of Sciences of the United States of America*, 99(12), 7821–6. <http://doi.org/10.1073/pnas.122653799>

Glasser, M. F., Coalson, T. S., Robinson, E. C., Hacker, C. D., Harwell, J., Yacoub, E., ... Van Essen, D. C. (2016). A multi-modal parcellation of human cerebral cortex. *Nature*, 536(7615), 171–178. <http://doi.org/10.1038/nature18933>

Gotham, K., Risi, S., Pickles, A., & Lord, C. (2007). The autism diagnostic observation schedule: Revised algorithms for improved diagnostic validity. *Journal of Autism and Developmental Disorders*, 37(4), 613–627. <http://doi.org/10.1007/s10803-006-0280-1>

Grady, C. L., Protzner, A. B., Kovacevic, N., Strother, S. C., Afshin-Pour, B., Wojtowicz, M., ... McIntosh, A. R. (2010). A multivariate analysis of age-related differences in default mode and task-positive networks across multiple cognitive domains. *Cerebral Cortex*, 20(6), 1432–1447. <http://doi.org/10.1093/cercor/bhp207>

Greicius, M. D., Krasnow, B., Reiss, A. L., & Menon, V. (2003). Functional connectivity in the resting brain: A network analysis of the default mode hypothesis. *Proceedings of the National Academy of Sciences of the United States of America*, 100(1), 253–8. <http://doi.org/10.1073/pnas.0135058100>

Herbert, M. R., Harris, G. J., Adrien, K. T., Ziegler, D. A., Makris, N., Kennedy, D. N., ... Caviness, V. S. (2002). Abnormal asymmetry in language association cortex in autism. *Annals of Neurology*, 52(5), 588–596. <http://doi.org/10.1002/ana.10349>

- Hillary, F. G., Medaglia, J. D., Gates, K. M., Molenaar, P. C., & Good, D. C. (2014). Examining network dynamics after traumatic brain injury using the extended unified SEM approach. *Brain Imaging and Behavior*, 8, 435–445. <http://doi.org/10.1007/s11682-012-9205-0>
- Jeste, S. S., & Geschwind, D. H. (2014). Disentangling the heterogeneity of autism spectrum disorder through genetic findings. *Nature Reviews Neurology*, 10(2), 74–81. <http://doi.org/10.1038/nrneurol.2013.278>
- Karalunas, S. L., Fair, D., Musser, E. D., Aykes, K., Iyer, S. P., & Nigg, J. T. (2014). Subtyping attention-deficit/hyperactivity disorder using temperament dimensions. *JAMA Psychiatry*, 71(9), 1015. <http://doi.org/10.1001/jamapsychiatry.2014.763>
- Karunanayaka, P., Eslinger, P. J., Wang, J.-L., Weitekamp, C. W., Molitoris, S., Gates, K. M., ... Yang, Q. X. (2014). Networks involved in olfaction and their dynamics using independent component analysis and unified structural equation modeling. *Human Brain Mapping*, 35, 2055–2072. <http://doi.org/10.1002/hbm.22312>
- Kennedy, D. P., Redcay, E., & Courchesne, E. (2006). Failing to deactivate: Resting functional abnormalities in autism. *Proceedings of the National Academy of Sciences*, 103(21), 8275–8280. <http://doi.org/10.1073/pnas.0600674103>
- Kim, J., Zhu, W., Chang, L., Bentler, P. M., & Ernst, T. (2007). Unified structural equation modeling approach for the analysis of multisubject, multivariate functional MRI data. *Human Brain Mapping*, 28(2), 85–93. <http://doi.org/10.1002/hbm.20259>
- Laird, A. R., Eickhoff, S. B., Li, K., Robin, D. A., Glahn, D. C., & Fox, P. T. (2009). Investigating the functional heterogeneity of the default mode network using

- coordinate-based meta-analytic modeling. *Journal of Neuroscience*, 29(46), 14496–14505. <http://doi.org/10.1523/JNEUROSCI.4004-09.2009>
- Lane, S. T., & Gates, K. M. (2017). Evaluating the use of the automated unified structural equation model for daily diary data. *Multivariate Behavioral Research*, 52(1), 126–127. <http://doi.org/10.1080/00273171.2016.1265439>
- Lane, S. T., Gates, K. M., & Molenaar, P. C. (2015). *gimme*. Retrieved from <https://cran.r-project.org/web/packages/gimme/index.html>
- Leitner, Y. (2014). The co-occurrence of autism and attention deficit hyperactivity disorder in children - what do we know? *Frontiers in Human Neuroscience*, 8, 268. <http://doi.org/10.3389/fnhum.2014.00268>
- Lenroot, R. K., & Yeung, P. K. (2013). Heterogeneity within Autism Spectrum Disorders: What have we learned from neuroimaging studies? *Frontiers in Human Neuroscience*, 7, 733. <http://doi.org/10.3389/fnhum.2013.00733>
- Lord, C., Rutter, M., DiLavore, P. C., Risi, S., Gotham, K., & Bishop, S. (2012). *Autism diagnostic observation schedule: ADOS-2*. Los Angeles, CA: Western Psychological Services.
- Lord, C., Rutter, M., & Le Couteur, A. (1994). Autism Diagnostic Interview-Revised: A revised version of a diagnostic interview for caregivers of individuals with possible pervasive developmental disorders. *Journal of Autism and Developmental Disorders*, 24(5), 659–685. <http://doi.org/10.1007/BF02172145>
- Lynch, C. J., Uddin, L. Q., Supekar, K., Khouzam, A., Phillips, J., & Menon, V. (2013).

- Default mode network in childhood autism: Posteromedial cortex heterogeneity and relationship with social deficits. *Biological Psychiatry*, 74(3), 212–219.  
<http://doi.org/10.1016/j.biopsych.2012.12.013>
- Marton, I., Wiener, J., Rogers, M., Moore, C., & Tannock, R. (2009). Empathy and social perspective taking in children with attention-deficit/hyperactivity disorder. *Journal of Abnormal Child Psychology*, 37(1), 107–18. <http://doi.org/10.1007/s10802-008-9262-4>
- McKeown, M. J., Makeig, S., Brown, G. G., Jung, T. P., Kindermann, S. S., Bell, A. J., & Sejnowski, T. J. (1998). Analysis of fMRI data by blind separation into independent spatial components. *Human Brain Mapping*, 6(3), 160–88.
- Menon, V. (2011). Large-scale brain networks and psychopathology: A unifying triple network model. *Trends in Cognitive Sciences*, 15(10), 483–506.  
<http://doi.org/10.1016/j.tics.2011.08.003>
- Meunier, D., Achard, S., Morcom, A., & Bullmore, E. (2009). Age-related changes in modular organization of human brain functional networks. *NeuroImage*, 44(3), 715–723. <http://doi.org/10.1016/j.neuroimage.2008.09.062>
- Milgram, S. (1967). The small world problem. *Psychology Today*, 1(1), 61–67.
- Miller, M. B., & Van Horn, J. D. (2007). Individual variability in brain activations associated with episodic retrieval: A role for large-scale databases. *International Journal of Psychophysiology*, 63(2), 205–213.  
<http://doi.org/10.1016/j.ijpsycho.2006.03.019>

- Miranda-Casas, A., Baixauli-Fortea, I., Colomer-Diago, C., & Roselló-Miranda, B. (2013). [Autism and attention deficit hyperactivity disorder: similarities and differences in executive functioning and theory of mind]. *Revista de Neurologia*, 57 Suppl 1, S177-84.
- Molenaar, P. C. M. (2015). On the relation between person-oriented and subject-specific approaches. *Journal for Person-Oriented Research*, 1(1–2), 34–41.  
<http://doi.org/10.17505/jpor.2015.04>
- Moreno-Alcázar, A., Ramos-Quiroga, J. A., Radua, J., Salavert, J., Palomar, G., Bosch, R., ... Pomarol-Clotet, E. (2016). Brain abnormalities in adults with Attention Deficit Hyperactivity Disorder revealed by voxel-based morphometry. *Psychiatry Research*, 254, 41–47. <http://doi.org/10.1016/j.psychresns.2016.06.002>
- Mumford, J. A., & Ramsey, J. D. (2014). Bayesian networks for fMRI: A primer. *NeuroImage*, 86, 573–582. <http://doi.org/10.1016/j.neuroimage.2013.10.020>
- Nacewicz, B. M., Dalton, K. M., Johnstone, T., Long, M. T., McAuliff, E. M., Oakes, T. R., ... Davidson, R. J. (2006). Amygdala volume and nonverbal social impairment in adolescent and adult males with autism. *Archives of General Psychiatry*, 63(12), 1417–28. <http://doi.org/10.1001/archpsyc.63.12.1417>
- Newman, M. E. J. (2004). Detecting community structure in networks. *European Physical Journal B*, 32(2), 321–330. <http://doi.org/10.1140/epjb/e2004-00124-y>
- Newman, M. E. J., Strogatz, S. H., & Watts, D. J. (2001). Random graphs with arbitrary degree distributions and their applications. *Physical Review E*, 64(2), 26118.  
<http://doi.org/10.1103/PhysRevE.64.026118>

Patriat, R., Molloy, E. K., Meier, T. B., Kirk, G. R., Nair, V. A., Meyerand, M. E., ...

Birn, R. M. (2013). The effect of resting condition on resting-state fMRI reliability and consistency: A comparison between resting with eyes open, closed, and fixated. *NeuroImage*, 78, 463–73. <http://doi.org/10.1016/j.neuroimage.2013.04.013>

Pelphrey, K. A., Morris, J. P., & McCarthy, G. (2005). Neural basis of eye gaze processing deficits in autism. *Brain*, 128(5), 1038–1048.  
<http://doi.org/10.1093/brain/awh404>

Plitt, M., Barnes, K. A., Wallace, G. L., Kenworthy, L., & Martin, A. (2015). Resting-state functional connectivity predicts longitudinal change in autistic traits and adaptive functioning in autism. *Proceedings of the National Academy of Sciences of the United States of America*, 112(48), E6699-706.  
<http://doi.org/10.1073/pnas.1510098112>

Price, R. B., Lane, S., Gates, K., Kraynak, T. E., Horner, M. S., Thase, M. E., & Siegle, G. J. (2016). Parsing heterogeneity in the brain connectivity of depressed and healthy adults during positive mood. *Biological Psychiatry*.  
<http://doi.org/10.1016/j.biopsych.2016.06.023>

Ramsey, J. D., Hanson, S. J., Hanson, C., Halchenko, Y. O., Poldrack, R. A., & Glymour, C. (2010). Six problems for causal inference from fMRI. *NeuroImage*, 49, 1545–1558. <http://doi.org/10.1016/j.neuroimage.2009.08.065>

Rojas, D. C., Peterson, E., Winterrowd, E., Reite, M. L., Rogers, S. J., & Tregellas, J. R. (2006). Regional gray matter volumetric changes in autism associated with social and repetitive behavior symptoms. *BMC Psychiatry*, 6(1), 56.

<http://doi.org/10.1186/1471-244X-6-56>

Rommelse, N. N. J., Franke, B., Geurts, H. M., Hartman, C. A., & Buitelaar, J. K. (2010).

Shared heritability of attention-deficit/hyperactivity disorder and autism spectrum disorder. *European Child & Adolescent Psychiatry*, 19(3), 281–95.

<http://doi.org/10.1007/s00787-010-0092-x>

Rommelse, N. N. J., Geurts, H. M., Franke, B., Buitelaar, J. K., & Hartman, C. A. (2011).

A review on cognitive and brain endophenotypes that may be common in autism spectrum disorder and attention-deficit/hyperactivity disorder and facilitate the search for pleiotropic genes. *Neuroscience and Biobehavioral Reviews*, 35(6), 1363–96. <http://doi.org/10.1016/j.neubiorev.2011.02.015>

Satterthwaite, T. D., Wolf, D. H., Loughead, J., Ruparel, K., Elliott, M. A., Hakonarson,

H., ... Gur, R. E. (2012). Impact of in-scanner head motion on multiple measures of functional connectivity: Relevance for studies of neurodevelopment in youth.

*NeuroImage*, 60(1), 623–632. <http://doi.org/10.1016/j.neuroimage.2011.12.063>

Schatz, A. M., Weimer, A. K., & Trauner, D. A. (2002). Brief report: attention

differences in Asperger syndrome. *Journal of Autism and Developmental Disorders*, 32(4), 333–6.

Schulte-Rüther, M., Greimel, E., Markowitsch, H. J., Kamp-Becker, I., Remschmidt, H.,

Fink, G. R., & Piefke, M. (2011). Dysfunctions in brain networks supporting empathy: An fMRI study in adults with autism spectrum disorders. *Social*

*Neuroscience*, 6(1), 1–21. <http://doi.org/10.1080/17470911003708032>

Schumann, C. M., Barnes, C. C., Lord, C., & Courchesne, E. (2009). Amygdala

- enlargement in toddlers with autism related to severity of social and communication impairments. *Biological Psychiatry*, 66(10), 942–949.  
<http://doi.org/10.1016/j.biopsych.2009.07.007>
- Seeley, W. W., Menon, V., Schatzberg, A. F., Keller, J., Glover, G. H., Kenna, H., ... Greicius, M. D. (2007). Dissociable intrinsic connectivity networks for salience processing and executive control. *Journal of Neuroscience*, 27(9).
- Shafritz, K. M., Dichter, G. S., Baranek, G. T., & Belger, A. (2008). The neural circuitry mediating shifts in behavioral response and cognitive set in autism. *Biological Psychiatry*, 63(10), 974–980. <http://doi.org/10.1016/j.biopsych.2007.06.028>
- Sharp, S. I., McQuillin, A., & Gurling, H. M. D. (2009). Genetics of attention-deficit hyperactivity disorder (ADHD). *Neuropharmacology*, 57(7–8), 590–600.  
<http://doi.org/10.1016/j.neuropharm.2009.08.011>
- Shirer, W. R., Ryali, S., Rykhlevskaia, E., Menon, V., & Greicius, M. D. (2012). Decoding subject-driven cognitive states with whole-brain connectivity patterns. *Cerebral Cortex*, 22(1), 158–65. <http://doi.org/10.1093/cercor/bhr099>
- Sidlauskaite, Sonuga-Barke, E., Roeyers, H., & Wiersema, J. R. (2016a). Altered intrinsic organisation of brain networks implicated in attentional processes in adult attention-deficit/hyperactivity disorder: A resting-state study of attention, default mode and salience network connectivity. *European Archives of Psychiatry and Clinical Neuroscience*, 266(4), 349–57. <http://doi.org/10.1007/s00406-015-0630-0>
- Sidlauskaite, Sonuga-Barke, E., Roeyers, H., & Wiersema, J. R. (2016b). Default mode network abnormalities during state switching in attention deficit hyperactivity



disorder. *Psychological Medicine*, 46(3), 519–28.

<http://doi.org/10.1017/S0033291715002019>

Simonoff, E., Pickles, A., Charman, T., Chandler, S., Loucas, T., & Baird, G. (2008).

Psychiatric disorders in children with autism spectrum disorders: Prevalence, comorbidity, and associated factors in a population-derived sample. *Journal of the American Academy of Child and Adolescent Psychiatry*, 47(8), 921–9.

<http://doi.org/10.1097/CHI.0b013e318179964f>

Smith, S. M. (2012). The future of fMRI connectivity. *NeuroImage*, 62, 1257–1266.

<http://doi.org/10.1016/j.neuroimage.2012.01.022>

Smith, S. M., Jenkinson, M., Woolrich, M. W., Beckmann, C. F., Behrens, T., Johansen-

Berg, H., ... Matthews, P. M. (2004). Advances in functional and structural MR image analysis and implementation as FSL. *NeuroImage*, 23(S1), 208–219.

Szatmari, P. (1999). Heterogeneity and the genetics of autism. *Journal of Psychiatry &*

*Neuroscience : JPN*, 24(2), 159–65.

Tzourio-Mazoyer, N., Landeau, B., Papathanassiou, D., Crivello, F., Etard, O., Delcroix,

N., ... Joliot, M. (2002). Automated anatomical labeling of activations in SPM

Using a macroscopic anatomical parcellation of the MNI MRI single-subject brain.

*NeuroImage*, 15(1), 273–289. <http://doi.org/10.1006/nimg.2001.0978>

Uddin, L. Q., Supekar, K., Lynch, C. J., Khouzam, A., Phillips, J., Feinstein, C., ...

Menon, V. (2013). Salience network–based classification and prediction of symptom severity in children with autism. *JAMA Psychiatry*, 70(8), 869.

<http://doi.org/10.1001/jamapsychiatry.2013.104>

- Valera, E. M., Faraone, S. V., Murray, K. E., & Seidman, L. J. (2007). Meta-analysis of structural imaging findings in attention-deficit/hyperactivity disorder. *Biological Psychiatry*, *61*(12), 1361–1369. <http://doi.org/10.1016/j.biopsych.2006.06.011>
- van den Heuvel, M. P., & Hulshoff Pol, H. E. (2010). Exploring the brain network: A review on resting-state fMRI functional connectivity. *European Neuropsychopharmacology*, *20*(8), 519–534. <http://doi.org/10.1016/j.euroneuro.2010.03.008>
- van den Heuvel, M. P., & Sporns, O. (2011). Rich-club organization of the human connectome. *Journal of Neuroscience*, *31*(44).
- van der Meer, J. M. J., Oerlemans, A. M., van Steijn, D. J., Lappenschaar, M. G. A., de Sonnevile, L. M. J., Buitelaar, J. K., & Rommelse, N. N. J. (2012). Are autism spectrum disorder and attention-deficit/hyperactivity disorder different manifestations of one overarching disorder? Cognitive and symptom evidence from a clinical and population-based sample. *Journal of the American Academy of Child and Adolescent Psychiatry*, *51*(11), 1160–1172.e3. <http://doi.org/10.1016/j.jaac.2012.08.024>
- Van Dijk, K. R. A., Hedden, T., Venkataraman, A., Evans, K. C., Lazar, S. W., Buckner, R. L., ... Milham, M. (2010). Intrinsic functional connectivity as a tool for human connectomics: theory, properties, and optimization. *Journal of Neurophysiology*, *103*(1), 297–321. <http://doi.org/10.1152/jn.00783.2009>
- Van Dijk, K. R. A., Sabuncu, M. R., & Buckner, R. L. (2012). The influence of head motion on intrinsic functional connectivity MRI. *NeuroImage*, *59*(1), 431–438.

<http://doi.org/10.1016/j.neuroimage.2011.07.044>

Wåhlstedt, C., Thorell, L. B., & Bohlin, G. (2009). Heterogeneity in ADHD:

Neuropsychological pathways, comorbidity and symptom domains. *Journal of Abnormal Child Psychology*, 37(4), 551–64. <http://doi.org/10.1007/s10802-008-9286-9>

Wang, L., Zhu, C., He, Y., Zang, Y., Cao, Q., Zhang, H., ... Wang, Y. (2009). Altered small-world brain functional networks in children with attention-deficit/hyperactivity disorder. *Human Brain Mapping*, 30(2), 638–649.

<http://doi.org/10.1002/hbm.20530>

Washington, S. D., Gordon, E. M., Brar, J., Warburton, S., Sawyer, A. T., Wolfe, A., ...

VanMeter, J. W. (2014). Dysmaturation of the default mode network in autism. *Human Brain Mapping*, 35(4), 1284–1296. <http://doi.org/10.1002/hbm.22252>

Wechsler, D. (1999). *Wechsler Abbreviated Scale of Intelligence (WASI)*. San Antonio, TX: The Psychological Corporation.

Wechsler, D. (2003). *Wechsler Intelligence Scale for Children-WISC-IV*. Psychological Corporation.

Willcutt, E. G. (2012). The prevalence of DSM-IV attention-deficit/hyperactivity disorder: A meta-analytic review. *Neurotherapeutics : The Journal of the American Society for Experimental NeuroTherapeutics*, 9(3), 490–9. <http://doi.org/10.1007/s13311-012-0135-8>

Yerys, B. E., Gordon, E. M., Abrams, D. N., Satterthwaite, T. D., Weinblatt, R.,


- Jankowski, K. F., ... Vaidya, C. J. (2015). Default mode network segregation and social deficits in autism spectrum disorder: Evidence from non-medicated children. *NeuroImage: Clinical*, 9, 223–232. <http://doi.org/10.1016/j.nicl.2015.07.018>
- Yerys, B. E., Wallace, G. L., Sokoloff, J. L., Shook, D. A., James, J. D., & Kenworthy, L. (2009). Attention deficit/hyperactivity disorder symptoms moderate cognition and behavior in children with autism spectrum disorders. *Autism Research : Official Journal of the International Society for Autism Research*, 2(6), 322–33. <http://doi.org/10.1002/aur.103>
- Zelle, S. L., Gates, K. M., Fiez, J. A., Sayette, M. A., & Wilson, S. J. (2016). The first day is always the hardest: Functional connectivity during cue exposure and the ability to resist smoking in the initial hours of a quit attempt. *NeuroImage*. <http://doi.org/10.1016/j.neuroimage.2016.03.015>

APPENDIX  
IRB APPROVAL FORM

DATE: December 12, 2016

**MEMORANDUM**

TO: Melissa Thye, PhD  
Principal Investigator

FROM: Cari Oliver, CIP   
Assistant Director  
Institutional Review Board for Human Use (IRB)

RE: Request for Determination – Not Human Subjects Research  
IRB Protocol N161130004 – **An Investigation of the Neurobiological  
Heterogeneity in Autism, ADHD, and Typical Development**

A member of the Office of the IRB has reviewed your Application for Not Human Subjects Research Designation for above referenced proposal.

The reviewer has determined that this proposal is **not** subject to FDA regulations and is **not** Human Subjects Research. Note that any changes to the project should be resubmitted to the Office of the IRB for determination.

470 Administration Building  
701 20th Street South  
205.934.3789  
Fax 205.934.1301  
irb@uab.edu

The University of  
Alabama at Birmingham  
Mailing Address:  
AB 470  
1720 2ND AVE S  
BIRMINGHAM AL 35294-0104